Ecological Informatics 26 (2015) 70–89

Contents lists available at ScienceDirect

Ecological Informatics

journal homepage: www.elsevier.com/locate/ecolinf

Towards the development of a biogeochemical model for addressing the eutrophication problems in the shallow hypertrophic lagoon of Albufera de Valencia, Spain

Gabriela Onandia [a,*], Alexey Gudimov [b], Maria Rosa Miracle [a], George Arhonditsis [b]

[a] Department of Microbiology and Ecology, ICBiBE, University of Valencia, E-46100 Burjassot, Valencia, Spain
[b] Ecological Modeling Laboratory, Department of Physical & Environmental Sciences, University of Toronto, Toronto, Ontario, Canada M1C 1A4

ARTICLE INFO

Article history:
Received 23 September 2014
Received in revised form 22 December 2014
Accepted 21 January 2015
Available online 29 January 2015

Keywords:
Eutrophication
macrophytes
nutrient recycling
sediment diagenesis
alternative states
lagoons

ABSTRACT

Our study presents a biogeochemical model that aims to reproduce the ecological processes shaping phytoplankton dynamics in the shallow hypertrophic lagoon of Albufera de Valencia (Spain). The model simulates two elemental cycles (N and P), two phytoplankton groups (cyanobacteria and non-cyanobacteria), and heterotrophic bacteria. First, we examine the capacity to reproduce the observed plankton patterns, while accommodating the uncertainty related to the external forcing factors of our model (hydraulic and nutrient loading, zooplankton grazing). Sensitivity analysis is also performed to identify the most influential parameters and therefore to shed light on the knowledge needed to solidify the model parameter specification. We subsequently utilize the calibrated model to assess the phytoplankton response to potential restoration actions; namely, the interplay between external nutrient loading reductions and variant flushing rates. The model successfully simulates a number of relevant water quality variables in the system, including total chlorophyll *a*, nitrate, ammonia, total nitrogen and total phosphorus. According to our sensitivity analysis, the credibility of the model as a management tool is primarily dependent upon the characterization of the phytoplankton growth strategies and associated settling rates. External P and N loadings are identified as the predominant driver of the system dynamics and their control should remain the main priority of local management efforts. Finally, we pinpoint future research directions that could advance our understanding of the ecosystem functioning, including an improved quantitative description of the seasonal variability of the hydraulic regime in the studied lagoon.

1. Introduction

Shallow lakes are the most abundant lake type at the global scale (Wetzel, 1990). The lack of stratification during extended periods in the summer and the tight water column-sediment coupling are predominant features of this type of water bodies (Scheffer et al., 1993). Many of these systems support significant economical and recreational activities, such as agriculture, fishing, bird watching, boating or tourism (McNeary and Erickson, 2013; Postel and Carpenter, 1997). However, an increasing number of shallow lakes worldwide has been subject to a variety of degradation processes, with the most profound being the cultural eutrophication (Dodds et al., 2008; Smith, 2003). The ramifications of shallow lake eutrophication usually comprise a wide range of detrimental changes in the food web structure and water biogeochemistry, but possibly the most conspicuous effects are the reduction in water transparency, the excessive increase in primary productivity, and the increased frequency of algal blooms, usually dominated by cyanobacteria that may be toxic or inedible (Carpenter et al., 1998; Smith et al., 2006).

The control of phosphorus (P) and nitrogen (N) exogenous loading has been shown to effectively alleviate the severity of eutrophication (Jeppesen et al., 2005; Schindler, 2006). In shallow lakes though, where the sediment surface to water volume ratio is high, the intense sediment-water column interplay aggravates the eutrophication problem and (most importantly) results in a considerable time lag in their response to the reduction of external nutrient loading (Søndergaard et al., 2003). Sediment resuspension, driven by both wind action and bioturbation, is responsible for a sizable reflux of nutrients into the water column. Likewise, the elevated amount of P retained in the sediments is subject to diagenesis processes and gets mobilized to the interstitial waters as phosphate, subsequently returning into the water column through Fickian diffusive transport (Søndergaard et al., 2003). Many of the associated sediment processes (e.g., bacteria-mediated mineralization) display seasonal variation, with their maximal rates typically observed during the summer period when the highest water temperatures occur (Søndergaard et al., 2003). Alongside with the P control, recent studies have also emphasized the importance of reducing N loading in temperate shallow lakes. For example, high N ambient levels can prevent the establishment of a clear-water state in shallow temperate lakes at moderately high ambient TP, but may play a lesser

* Corresponding author. Tel.: +34 963544616.
E-mail address: gabriela.onandia@uv.es (G. Onandia).

http://dx.doi.org/10.1016/j.ecoinf.2015.01.004
1574-9541/

role at very low TP concentrations (González Sagrario et al., 2005). Likewise, low nitrogen availability has been identified as a critical condition for the maintenance of macrophyte dominance at intermediate to high TP levels in the shallow Mediterranean Lake Eymir, Turkey (Beklioglu et al., 2003). Thus, recognizing the uncertainty of restoration efforts that solely focus on external nutrient loading reductions, the contemporary eutrophication management paradigm has evolved to include biological or hydrological manipulations as complementary strategies to accelerate system restoration (Gulati and van Donk, 2002). For example, early work highlighted the importance of the causal linkage between water residence time and phytoplankton productivity or other eutrophication symptoms (Dickman, 1969; Dillon, 1975). Since then, numerous studies have described a negative relationship between flushing rates and phytoplankton biomass in eutrophic shallow lakes, pinpointing the reduction of water residence time by flushing as a potentially effective restoration action (Jagtman et al., 1992; Moustaka-Gouni et al., 2006; Padisák et al., 1999).

According to the alternative stable states theory, shallow eutrophic lakes can oscillate between two alternative equilibria: a clear water state characterized by high water transparency and submerged macrophyte vegetation, and a turbid state dominated by phytoplankton with little or absent macrophyte cover (Scheffer et al., 1993). Albufera de Valencia, a warm-temperate shallow oligohaline lagoon, was populated by rich submerged vegetation during the first half of the 20th century (Pardo, 1942). Following intense eutrophication processes throughout the 1960s, the system shifted from a clear into a turbid stable state which was consolidated by the virtual disappearance of macrophytes in the early 1970s (Vicente and Miracle, 1992). The latter turbid state has prevailed since then, although short-term clear-water events, with chlorophyll *a* concentrations below 5 μg L^{-1}, intermittently offer a different perspective of the dynamics of this shallow coastal lagoon (Miracle and Sahuquillo, 2002; Romo et al., 2005). These events are largely dependent upon the hydrological regime and are characterized by a drastic increase in water transparency which lasts for a short period (up to five weeks), reduction of phytoplankton biomass, and change in the plankton community composition, with decline of cyanobacteria and increase of chlorophyte and diatom abundance, concomitant to large cladocera (*Daphnia magna*) abundance increase (Onandia et al., 2014b; Sahuquillo et al., 2007).

Nonetheless, the short duration of these events, together with the lack of macrophyte resurgence, represent fundamental differences relative to the clear-water alternative stable states typically characterizing shallow lakes (Scheffer et al., 1993). Further, the timing and causes of clear-water events in Albufera de Valencia appear to differ from most descriptions in the limnological literature. In the majority of shallow eutrophic lakes, clear-water phases typically occur in spring and are triggered by zooplankton grazing (Dröscher et al., 2008; Lampert et al., 1986; Tõnno et al., 2003), although other factors such as climatic forcing could be relevant (Dröscher et al., 2009; Tirok and Gaedke, 2006). In Albufera de Valencia, clear-water phases are experienced in the winter and are mainly driven by a suite of factors, such as: i) the intense "flushing" induced by the draining of the rice paddies in the surrounding watershed, leading to the reduction of phytoplankton biomass by its direct export from the lagoon into the sea; *ii*) the mild water temperatures that enhance the net growth of *Daphnia magna*; and *iii*) a decrease in fish predation on zooplankton, stemming from the annual maximum catch rates by local fishermen during the same period (Romo et al., 2005). These factors, along with the low light availability and suboptimal water temperatures for algal growth, magnify the top-down control of phytoplankton biomass by herbivorous zooplankton. However, these favorable conditions do not last for long, very likely because of the intense fish predation on zooplankton exerted by *Liza aurata* Risso and *Cyprinus carpio* L. during the spring, which is a recurring pattern in subtropical and southern temperate shallow lakes and lagoons (Blanco et al., 2003; Romo et al., 2005 and references therein). Of equal importance is that the water flow through the lake is drastically reduced after the rice paddies are drained, favoring the re-establishment of cyanobacteria dominance.

In an attempt to improve the water quality of the lagoon, a sewage purification plan was implemented during the 1990s, resulting in a significant nutrient input reduction; namely, 77% in TP and 24% in TN (Romo et al., 2005). This improvement was translated into a notable reduction in chlorophyll *a* levels (from 270 to 180 μg L^{-1}), but cyanobacteria dominance still remains a thorny issue (Romo et al., 2005, 2008). More recently, several surface constructed wetlands have been developed (Tancat de la Pipa, Tancat de Mília and Estany de la Plana), but their current functioning does not necessarily maximize the removal of phytoplankton, phosphorus and nitrogen (Martín et al., 2013). Thus, in spite of all the management actions, the system arguably remains hypertrophic. According to the Ecoframe scheme (Moss et al., 2003), Albufera de Valencia is still in a bad ecological status and additional actions should be undertaken to ameliorate ecosystem recovery.

In this regard, the goal of the present modeling study is to reproduce the interplay among the ecological processes that shape the planktonic patterns in the coastal shallow lagoon of Albufera de Valencia. Ecological modeling represents a useful tool to elucidate the physical and biogeochemical processes underlying the local eutrophication problems and to design management plans that effectively balance between environmental concerns and local socioeconomic values (Usaquén Perilla et al., 2012). The N and P cycles as well as the dynamics of two phytoplankton groups (cyanobacteria and non-cyanobacteria) and heterotrophic bacteria are simulated by the model. We present the results of the calibration and validation exercise and examine the ability of the model to reproduce the observed plankton patterns in Albufera de Valencia, while accommodating the uncertainty of the external forcing factors. Sensitivity analysis is performed to identify the most influential parameters for the phytoplankton simulations. We conclude by pinpointing knowledge gaps and recommending future research directions.

2. Materials and Methods

2.1. Study Site-Data Collection

Albufera de Valencia is an oligohaline (salinity ≈ 1 ‰) lagoon located at the Mediterranean coast, 15 km south of the city of Valencia (Spain). It has a mean depth of ≈ 1 m and covers an area of approximately 24 km^2. This shallow system is currently characterized as hypertrophic, with average annual chlorophyll *a* levels of 167 μg L^{-1} (4 – 322 μg L^{-1}), Secchi disk depth of 0.34 m (0.18 – 1 m), total phosphorus (TP) of 155 μg L^{-1} (41 – 247 μg L^{-1}), and total nitrogen (TN) of 3.9 mg L^{-1} (1.8 – 6.6 mg L^{-1}). Similarly, the primary productivity is remarkably high, varying between 1 – 12 mg C m^{-2} d^{-1} (Onandia et al., 2014b). The lagoon is surrounded by a 223 km^2 area primarily used for rice cultivation. Numerous irrigation ditches cross the rice paddies and flow into the system, discharging nutrient and organic matter loadings. Three outlet channels or "golas" with sluices connect the lagoon with the Mediterranean Sea, separated only by a 500 — 1000 m wide sand bar, thereby allowing water level regulations. Thus, the water requirements of the rice culture predominantly shape the hydrological cycle of the lagoon. In mid-autumn, the rice paddies are flooded without culture. In the winter, there is a major period of high water renewal rate driven by the draining of the flooded paddies. During the spring period, the dry paddies are prepared for rice sowing in May; at that point, the paddies are flooded again, defining the beginning of a period of low water renewal rate that lasts throughout the rice growing season. Rice is harvested in late summer (mid-September) and thereafter, a secondary period (end of September - October) of moderately high water flow takes place until the paddies are flooded again. The lagoon, the surrounding paddies, and the sand bar, characterized by two parallel dunes covered by Mediterranean vegetation, form the "L'Albufera de Valencia Natural Park", which has been included in the Ramsar List of

Wetland of International Importance since 1990, and was subsequently designed as a Special Area for Bird Protection (ZEPA).

Based on previous studies of the relative contribution of the water masses in the ditches (Soria and Vicente, 2002; Vicente et al., 2012), twenty channels representing around 85% of the total inflows were selected to quantify the hydraulic and nutrient loading into the lagoon. Even though the outflows take place mainly through the "golas", certain incoming channels, such as Reina Nova and Reina Vella (Fig. 1), often change water flow direction behaving as outlet channels and were computed as such in those occasions. It should also be noted that the outflows through the "Perelló gola" were not taken into account. Firstly, because Reina Nova and Reina Vella channels discharge into this gola, when they function as outlet channels (and therefore computing the outflows through this gola would have led to an outflow overestimation), and secondly, because the "Perelló gola" collects water from sources other than the lagoon, namely from the rice paddies located in the south area. Water flow in the "golas" and selected channels was estimated during 2010-2011 with weekly to monthly frequency by measuring the cross-section and length of a stretch of the channel and then introducing Rhodamin-coloured waves into the stream to assess maximum water speed as described in Soria and Vicente (2002). These estimations also accounted for the different coating of the channels by correcting with Fisher's formula (Escribá, 1988). Additionally, we used daily flow data obtained with an acoustic Doppler current profiler in the main channels (Gola de Pujol, Perellonet, Reina Nova, Reina Vella, Overa and Dereta).These data were provided by the Confederación Hidrográfica del Jucar (Regional Basin Authority).

Water samples were collected during 2010-2011 at the selected channels, the "golas", and at four stations within the lagoon (Fig. 1) with weekly (during the clear-water event in 2010) to monthly frequency (with the exceptions of February 2010 and June 2011). Conductivity, pH, salinity, oxygen saturation (%), dissolved oxygen (mg DO L^{-1}) and temperature were measured *in situ* with a multiparameter WTW 350i probe. Physicochemical variables, such as water turbidity (WT), suspended solids (SS), ammonia (NH_4), nitrate (NO_3), nitrite (NO_2), TN, phosphate (PO_4). TP and alkalinity (Alk) were determined following the methodology described in APHA (1992). Dissolved and total organic and inorganic carbon (DOC, TOC, DIC, TIC) were measured with a Total Organic Carbon Analyzer (TOC-VCSH) by high temperature combustion, as described in ISO (1997). More details about the methodology used along with the general trends of the measured water quality variables can be found in Onandia et al., 2014a,2014b. Additionally, vertical profiles of photosynthetic active radiation (PAR) were measured at the sampling stations in the lagoon with a 2π quantum sensor (Li-192SA) attached to a LiCor Li-1000 data logger. The acquired values (at 0.1 m depth intervals) were used to derive the vertical light attenuation coefficient (K_d) of PAR. Secchi disk depth was also recorded.

Chlorophyll *a* collected onto glass fiber filters (GF/F, Whatman) was measured spectrophotometrically as described in Shoaf and Lium (1976). The biomass of the different phytoplankton groups was also

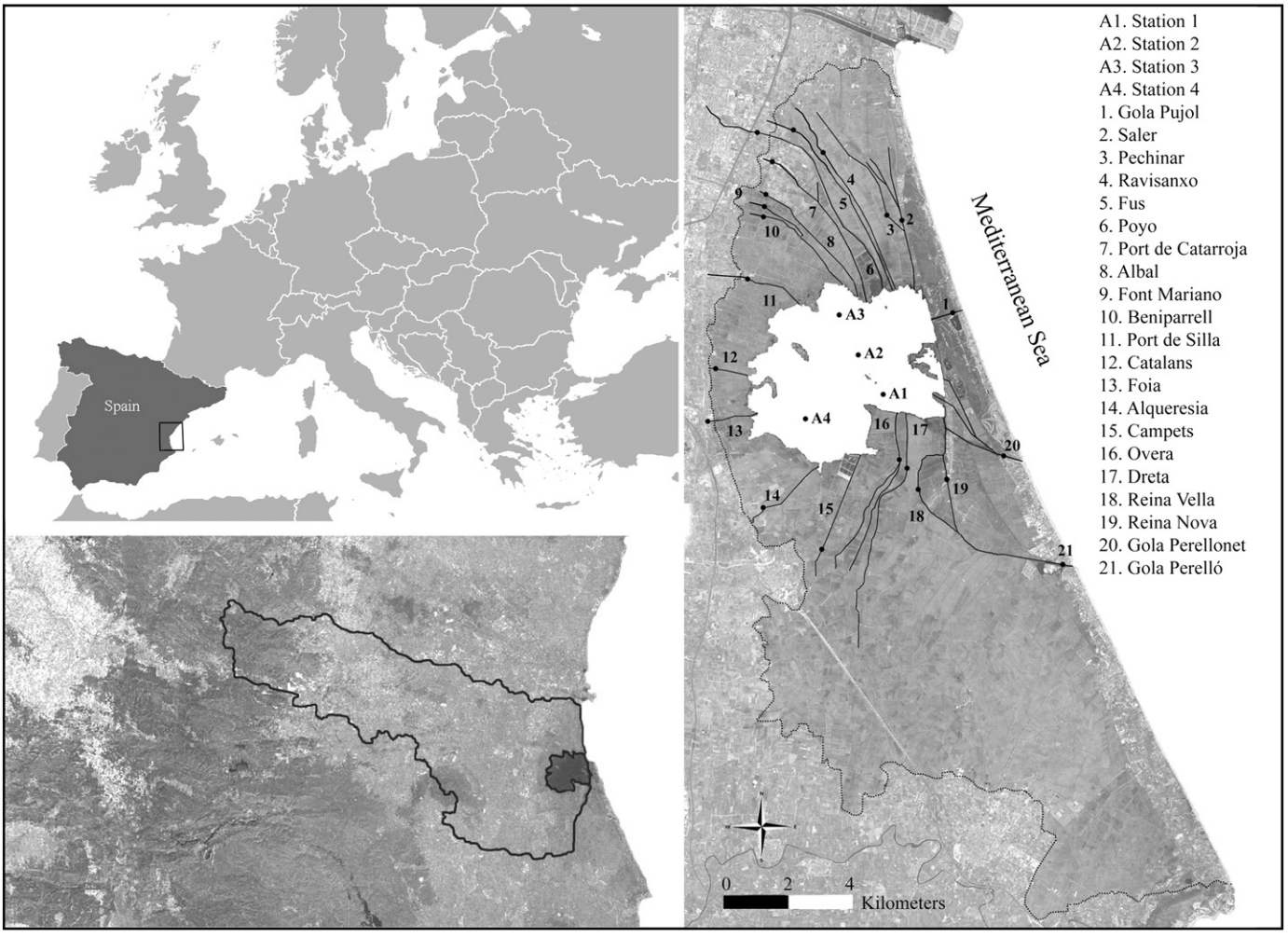

Fig. 1. Map of Albufera de Valencia, with monitored channels and sampling locations. The limits of "L'Albufera de Valencia Natural Park" (dotted line) are also shown along with the lagoon watershed (solid line).

estimated. DAPI-stained bacteria samples were counted under a epifluorescence microscope (Zeiss III RS) and cell volume was estimated based on measurements of dimensions in microphotographs using the general Sommaruga (1995) formula. Cell carbon content was then derived by applying a conversion factor of 0.2 pg C μm^{-3} (Simon and Azam, 1989). Samples for algal cell counts were preserved in Lugol solution and enumerated with an inverted microscope at 1000X in a 3 mL sedimentation chamber. Cell biovolume was calculated as described by Hillebrand et al. (1999) and cell carbon was subsequently estimated using a conversion factor of 0.225 pg C μm^{-3} for mixed phytoplankton populations (Reynolds, 1984). Zooplankton samples were concentrated by filtering with a 30 μm mesh nytal filter, preserved with formalin 4%, and counted with an inverted microscope at 100x magnification. Zooplankton biomass was obtained using species-specific dry weight conversion factors (Bottrell, 1976; Dumont et al., 1975; Latja and Salonen, 1978; Telesh et al., 1998).

2.2. Model description

2.2.1. Model structure and forcing functions

In this section, we present the basic conceptual design of the model. The model equations are shown in Table 1 and the definitions of model parameters are presented in Table 2. The present ecological model is partly based on the eutrophication model of Lake Washington developed by Arhonditsis and Brett (2005a, 2005b). Given the shallowness of the system (mean depth ≈ 1 m) and thus the lack of vertical stratification, the model consists of only one spatial compartment. The model considers the interactions among the following state variables: nitrate, ammonium, organic nitrogen, phosphate, organic phosphorus, detritus, bacteria and two phytoplankton groups: cyanobacteria and non-cyanobacteria. Our data on total zooplankton biomass and community composition provided evidence of two very distinct zooplankton characterizations. The first one corresponds to the period in which cladocera dominated the zooplankton community; namely, the clear-water event observed in late winter of 2010. The second corresponds to the zooplankton community observed during most of the study period, dominated by copepods (*Acanthocyclops americanus*), rotifers (*Brachionus calyciflorus*, *Brachionus angularis*, *Keratella tropica*, *Keratella cochlearis* or *Polyarthra* sp.) as well as small-sized cladocera (e.g., *Bosmina longirostris*, *Ceriodaphnia* sp., *Alona* sp., *Chydorus* sp., and *Moina* sp.). However, while the representation of zooplankton as one aggregated entity was clearly inadequate, the available empirical information was insufficient to credibly parameterize two zooplankton functional groups and subsequently test them in the extrapolation model domain; that is, the validation dataset did not include a clear-water event to test the robustness of a "cladocera-like" group (see following Results). Based on this limitation, the role of zooplankton in the system was accounted for by including it as an external forcing function, i.e., we do not explicitly consider zooplankton as a state variable, but rather the model is externally forced with the observed zooplankton biomass data.

Other external forcing functions include water temperature, solar radiation, dissolved oxygen, light extinction coefficient, day length, precipitation, evaporation, wind, atmospheric deposition, channel inflows/outflows, and the associated nutrient loading. Water temperature, solar radiation and dissolved oxygen were approximated by sinusoidal functions, based on our field measurements. Given the absence of data closer to the system, day length, precipitation, evaporation and wind forcing were based on the Valencia Airport weather station (≈20 km from La Albufera de Valencia) provided by the Meteorological State Agency (AEMET). Although the distance of the wind speed data from the lagoon might introduce uncertainty into our modelling exercise, we believe that the flat topography of the area minimizes the likelihood of a major error with our wind-resuspension estimates. Precipitation and evaporation data as well as inflows and outflows were used to calculate the water budget of the system, and thus explicitly account for the seasonal variability in the lagoon volume. Daily data on outflows and water level variations were provided by the Confederación Hidrográfica del Júcar. Based on daily outflow measurements, we adjusted our inflow estimates in order to fit water level changes in the lagoon. The flushing rate was estimated to be 8.9 y^{-1}, which is somewhat lower comparing with the value (9.8 y^{-1}) reported for 1988 (Soria and Vicente, 2002). The Albufera de Valencia 971.1 km^2 watershed hosts industrial and agricultural activities as well as a fairly dense population (Soria and Vicente, 2002). Water sources include groundwater springs ("ullals") and natural runoff, but also treated sewage from domestic and industrial origin (containing a small untreated fraction) and surplus agricultural water. The external nutrient loading cycle was based on flow-weighted nutrient concentrations measured for the selected tributaries (Fig. 2). Atmospheric NO_3 and NH_4 deposition is based on bulk deposition values from El Saler, a village located 4 km north from the lagoon (Sanz et al., 2002). PO_4 data are based on dissolved inorganic phosphorus bulk deposition for the southwestern Mediterranean (Morales-Baquero et al., 2006).

2.2.2. Model Equations

2.2.2.1. Phytoplankton. The phytoplankton of Albufera de Valencia has been extensively studied over the last 40 years (García et al., 1984; Romo et al., 2008; Romo and Miracle, 1994, 1995; Villena and Romo, 2003; Vicente and Miracle 1992). While there have been noticeable changes in the phytoplankton community composition over time, the total biomass and chlorophyll *a* levels consistently reflect the shift of the lagoon into a hypertrophic state. Detailed description of the current phytoplankton seasonal succession patterns can be found in Onandia et al., 2014b. Briefly, the flow rate increase during the winter draining of the rice paddies brings a substantial improvement of the water transparency, which in turn results in a decrease of cyanobacteria biomass and a greater relative contribution from cryptophytes (*Cryptomonas* sp. and *Rhodomonas* sp.), chrysophytes (*Chrysochromulina* sp., *Prymnesium* sp.) and diatoms (*Cyclotella* sp., *Nitzschia* sp and *Fragilaria* sp). In the spring, the flow through the lagoon is reduced and the water column stability is re-established. Diatoms (*Fragilaria* sp.) and cyanobacteria (*Pseudanabaena galeata*, *Merismopedia* sp. pl.) dominate the algal assemblage. Phytoplankton growth displays a nearly monotonic increase throughout the spring attaining its annual maximum biomass towards the end of the season. In the summer period, cyanobacteria represent up to ≈ 90% of the total phytoplankton biomass, with common species such as *Planktolyngbya* sp., *Aphanothece* sp., *Merismopedia* sp. or the heterocystous cyanobacterium *Cylindrospermopsis raciborskii*.

Based on this seasonal phytoplankton succession pattern, we opted for the simulation of two phytoplankton groups that differ in regard to their strategies for resource competition (nitrogen, phosphorus, light and temperature), metabolic rates, morphological features (settling velocity, shading effects) and palatability for zooplankton. Cyanobacteria are modeled as K strategist, with low maximum growth rates and mortality, fast nitrogen and slow phosphorus kinetics, high tolerance to low light availability, high temperature optima, low settling velocity and low edibility as food source for zooplankton. By contrast, the more generic "non-cyanobacteria" group has attributes of r-selected organisms with high maximum growth rates and higher metabolic losses, relatively fast phosphorus and slow nitrogen kinetics, low temperature optima, high sinking velocities and high palatability for zooplankton. This group aims to feature the properties of the spring phytoplankton community (with an important contribution of diatoms) as well as the winter algal assemblage (dominated by chlorophytes, chrysophytes and diatoms).

The phytoplankton equation considers biomass production and losses due to mortality, settling, zooplankton grazing, and outflows from the lagoon. The influence of temperature, light, and nutrient availability on phytoplankton is mathematically represented by the multiplicative model (Cerco and Cole, 1994). Phosphorus and nitrogen dynamics within the phytoplankton cells account for luxury uptake (Arhonditsis et al., 2002; Hamilton and Schladow, 1997). Phytoplankton

Table 1
Mathematical equations of the eutrophication model for the Albufera de Valencia lagoon.

No.	State Variable	Term	Equation
1	**Phytoplankton biomass**	$\frac{dPHYT_{i,x}}{dt}$	$= growth_{i,x} \times PHYT_{i,x} - mp_i \times e^{kt(Tx\text{-}Tempref)} \times PHYT_{i,x}$ $- Vsettling_i \times PHYT_{i,x}/z_x - Grazing_{i,x} \times ftemperature_x \times ZOOP_x$ $- outflows \times PHYT_{i,x}$,where
	Growth rate	$growth_{i,x}$	$= gwthmax_i \times fnutrient_{i,x} \times flight_{i,x} \times ftemperature_{i,x}$
	Nutrient limitation	$fnutrient_{i,x}$	$= min\{\varphi IN_{i,x}, \varphi PO4_{i,x}\}$
	Phosphate limitation	$\varphi PO4_{i,x}$	$= (Pint_{i,x} - Pmin_i)/(Pmax_i - Pmin_i)$
	Intracellular phosphorus content	$\frac{dPint_{i,x}}{dt}$	$= Pup_{i,x} \times Pfb_{i,x} - growth_{i,x} \times Pint_{i,x}$
	Nitrogen limitation	$\varphi IN_{i,x}$	$= (Nint_{i,x} - Nmin_i)/(Nmax_i - Nmin_i)$
	Intracellular Nitrogen content	$\frac{dNint_{i,x}}{dt}$	$= Nupi,x \times Nfbi,x - growth\ i,x \times Ninti,x$
	Phosphorus uptake	$Pup_{i,x}$	$= Pmaxuptake_i \times (PO4_x/(PO4_x + KP_i))$
	Nitrogen uptake	$Nup_{i,x}$	$= Nmaxuptake_i \times (IN_x/(IN_x + KN_i))$
	Feedback control	$Pfb_{i,x}$	$= (Pmax_i - Pint_{i,x})/(Pmax_i - Pmin_i)$
	Feedback control	$_{Nfbi,x}$	$= (Nmax_i - Nint_i)/(Nmax_i - Nmin_i)$
	Light limitation	$flight_{i,x}$	$= 2.718 \times (FD/(K_{dx} \times z_x)) \times (e^{-a1} - e^{-a0})$, where $a0_i = (I/Ik_i)$, $a1_i = (I/Ik_i)e^{(-kdx \times zx)}$
		FD	$=$ the fractional day length $(0 \le FD \le 1)$
	Light attenuation	K_{dx}	$= K_d b + K_d chla_i \times \sum_i PHYT_{i,x}/(C_i/Chl\alpha) + K_d SS \times SS$
	Temperature limitation	$ftemperature_{i,x}$	$= e^{(-KTgr\ (T_x - Trefi,x)^2)}$
2	**Zooplankton-related equations**		
	Grazing rate for phytoplankton	$Grazing_{i,x}$	$= maxgrazing \times (Pref_{i,x} \times PHYT_{i,x})/(KZ + Food_x)$
	Grazing rate for detritus	$Grazing_{det,x}$	$= maxgrazing \times (Pref_{det,x} \times Detritus_x)/(KZ + Food_x)$
	Grazing rate for bacteria	$Grazing_{bact,x}$	$= maxgrazing \times (Pref_{bact,x} \times BACT_x)/(KZ + Food_x)$
	Food abundance	$Food_x$	$= \sum_i Pref_{herb\ i,x} \times PHYT_{i,x} + Pref_{herbdet,x} \times Detritus_x + Pref_{herbact,x} \times BACT_x$
	Preference of zooplankton for phytoplankton *i*	$Pref_{i,x}$	$= (Pref_i \times PHYT_{i,x})/(\sum_i Pref_i \times PHYT_{i,x} + Pref_{det} \times Detritus_x + Pref_{bact} \times BACT_x)$
	Preference of zooplankton for detritus	$Pref_{det,x}$	$= (Pref_{det} \times Detritus_x)/(\sum_i Pref_i \times PHYT_{i,x} + Pref_{det} \times Detritus_x + Pref_{bact} \times BACT_x)$
	Preference of zooplankton for bacteria	$Pref_{bact,x}$	$= (Pref_{bact} \times BACT_x)/(\sum_i Pref_i \times PHYT_{i,x} + Pref_{det} \times Detritus_x + Pref_{bact} \times BACT_x)$
	Temperature limitation for growth	$ftemperature_x$	$= e^{(-KTgr1_{zoo}(T_x - Trefzoo)^2)}$ when $T < Trefzoo + e^{(-KTgr2_{zoo}(T_x - Trefzoo)^2)}$ when $T \ge Trefzoo$
3	**Bacteria**	$\frac{dBACT}{dt}$	$= uptake_{bact} \times BACT - mb \times \sigma_t \times BACT^{1.65} - Grazing_{bact,x} \times ftemperature_x \times ZOOP_x$, where
	Uptake rate	$uptake_{bact}$	$= (U_1 + U_2) \times \sigma_t$
	NH4 uptake	U_1	$= (Uptakemax_{bact} \times ON)/(DH + S + O)$
	DON uptake	U_2	$= (Uptakemax_{bact} \times S)/(DH + S + ON)$
	Total N substrate	S	$= \min(NH4, v \times ON)$
		σ_t	$= \left(1 - 0.5\cos\left(\frac{2\pi t(day)}{365}\right)\right)/(1 + 0.5)$
4	**Detritus concentration**	$\frac{dDetritus_x}{dt}$	$= \sum_i [(1 - \alpha_{DOC\ i}) \times mp_i \times e^{kt(Tx\text{-}Tempref)} \times PHYT_{i,x}] + [(1 - \alpha_{DOCzoo}) \times mz \times e^{kt(Tx\text{-}Tempref)} \times (ZOOP_x^2/(ZOOP_x^2 + Pred^2)) \times ZOOP_x] - [(maxgrazing \times Pref_{det,x} \times Detritus_x)/(KZ + Food_x)] \times ftemperature_x \times ZOOP_x$ $- Vsettling_{(biogenic)} \times Detritus_x/z_x - KCmineral_x \times Detritus_x$
	Carbon mineralization rate	$KCmineral_x$	$= ftemperature\_min_x \times KCrefmineral$, where
	Temperature limitation for mineralization	$ftemperature\_min_x$	$= e^{(-KTFmin(T_x - Toptmin)^2)}$
5	**Phosphate concentration**	$\frac{dPO_{4x}}{dt}$	$= -\sum_i Pup_{i,x} \times Pfb_{i,x} \times PHYT_{i,x} + \sum_i \alpha_{PO4\ i} \times mp_i \times e^{kt(Tx\text{-}Tempref)} \times Pint_{i,x} \times PHYT_{i,x} + \alpha_{PO4\ j} \times mz \times e^{kt(Tx\text{-}Tempref)} \times (ZOOP_x^2/(ZOOP_x^2 + Pred^2)) \times ZOOP_x \times PC_{zoo} + KPmineral_x \times OP_x + PO_4EXOG_x + PO_4ENDOG_x - Outflows \times PO4$, where
	Phosphorus mineralization rate	$KPmineral_x$	$= ftemperature\_min_x \times KPrefmineral$
		$ftemperature\_min_x$	$= e^{KTFmin\ (Tx\text{-}Tempref)}$
	Endogenous flux	PO_4ENDOG_x	$= PO_{4\ sed\ x}/z_x$
6	**Organic phosphorus concentration**	$\frac{dOP_x}{dt}$	$= DetritusP_x - DetritusGrazing\ P_x \times ftemperature_x \times ZOOP_x$ $- KPmineral_x \times OP_x + OPEXOG_x + OPENDO_x - Outflows \times OP - (Detritus\ P_x/OP_x \times Vbiosettling + (1\text{-}Detritus\ P_x/OP_x) \times Vsettling) \times OP_x/z_x$
	OP flux from sediment	$OPENDO_x$	$= TurbFish + \varepsilon OP + OPSED_x$
	Fish bioturbation	$TurbFish$	$= (Rresusfish \times fishbiomass \times ftemperature)$
	Relative resuspension by adult fish browsing	$Rresuspfish$	$= g\ sediment \times g\ dry\ weight\ fish^{-1}\ day^{-1}$
	Fish biomass per area	$fishbiomass$	$= g\ dry\ weight\ fish\ m^{-2}$
	Effects of temperature on fish bioturbation	$ftemperature$	$= e^{(-KTgr\ (T_x - Treffish)^2)}$
	Wind resuspension	εOP	$= \alpha_0 \times ((\sigma - \sigma_c)/\sigma_c)^b$ if $\sigma \ge \sigma_c$, 0 if $\sigma < \sigma_c$
	Rate of sediment release of organic phosphorus	$OPSED_x$	$= OPosed \times e^{(kt_{sed}(Tsed\text{-}Tempref_{sed})}$, where
		$OPosed$	$= 0.1\ mg\ m^{-2}\ day^{-1}$
	Biogenic organic phosphorus accumulation	$DetritusP_x$	$= \sum_i (1 - \alpha_{PO4\ i}) \times mp_i \times e^{kt(T_x\text{-}Tempref)} \times Pint_{i,x} \times PHYT_{i,x} + (1 - \alpha_{PO4\ zoo}) \times mz \times e^{kt(T_x\text{-}Tempref)} \times PC_{zoo} \times ZOOP_x$
	Loss due to zooplankton grazing upon detritus	$DetritusGrazingP_{j,x}$	$= (maxgrazing \times Pref_{det,x} \times DetritusP_x)/(KZ_j + Food_x)$
	Loss due to particulate phosphorus settling	$SettlingP_x$	$= (DetritusP_x/OP_x) \times Vsettling_{(biogenic)} + (1 - (DetritusP_x/OP_x)) \times Vsettling$
7	**Ammonium concentration**	$\frac{dNH_{4x}}{dt}$	$= -\sum_i prefNH4_{(i,x)} \times Nup_{i,x} \times Nfb_{i,x} \times PHYT_{i,x}$ $+ \sum_i \alpha NH4_i \times mp_i \times e^{kt(Tx\text{-}Tempref)} \times Ninti_x \times PHYT_{i,x}$

Table 1 (*continued*)

No.	State Variable	Term	Equation
			$+ aNH4_{zoo} \times mz_j \times e^{kt(Tx- Tempref)} \times (ZOOP_x^2/(ZOOP_x^2 + Pred^2) \times N/C_{zoo} \times ZOOP_x + \alpha_{bact} NH4_i \times mbact\ x_i \times \sigma_t \times BACT^{1.65} \times (N/C_{bact}) - U_2 \times \sigma_t \times BACT \times (N/C_{bact}) - Nitrification_x - Outflows \times NH4 + NH4EXOG_{EPI} + NH4ENDOG_x$
	Mineralization rate	$KNmineral_x$	$= KN_{refmineral} \times ftemperature\_min_x$
	Nitrification rate	$Nitrification_x$	$= Nitrifmax \times flightnitr_x \times (DO_x/(DO_x + KHdonit)) \times (NH4_x/(KHnh4nit + NH4_x)) \times ftempnitr_x$
	Light limitation	$flightnitr_x$	$= 1\ when\ I_x \le 0.1 \times I,\ else\ flightnitr_x = 0$
	Temperature limitation	$ftempnitr_x$	$= e^{(-KTFgrnitr(T_x\text{-}Toptnitr)^2)}$
	Intensity of light in compartment x	I_x	$= I/(K_{dx} \times z_x)(e^{-kd_x \times H_x} - e^{-kd_x \times (z_x + H_x)})$
	Nitrogen-to-carbon ratio of the zooplankton cells	N/C_j	$= 0.2$
	Nitrogen-to-carbon ratio of the bacteria cells	N/C_{bact}	$= 0.18$
	Endogenous flux	$NH4ENDOG_x$	$= NH_{4\ sed\ x}/z_x$
8	**Nitrate concentration**	$\frac{dNO_{3x}}{dt}$	$= \sum_i (1 - prefNH4_{(i,x)}) \times Nup_{i,x} \times Nfb_{i,x} \times PHYT_{i,x} + Nitrification_x - Denitrification_x - Outflows \times NO3 + NO3EXOG_x + NO3ENDOG_x;$
	Ammonium preference	$prefNH4$	$NH4/(NH4 + NO3)$
	Denitrification rate	$Denitrificationx$	$= Denitrifmax \times (KHdodenit/(DO_x + KHdodenit)) \times (NO3_x/(KHno3nit + NO3_x)) \times ftempdenitr_x$
	Nitrification rate	$Nitrificationx$	$Nitrifmax \times flightnitr(x) \times (NH4_x/(KHammonitr + NH4_X)) \times (DO_X/(KHoxygnitr + DO_X)) \times N\ ftempnitr(x)$
	Temperature limitation	$ftempdenitr_x$	$= e^{(-KTgrdenitr(T_x\text{-}Toptdenitr)^2)}$
9	**Organic nitrogen concentration**	$\frac{dON_x}{dt}$	$= Detritus\ N_x - \sum_i \text{DetritusGrazing N}_{j,x} \times \text{ftemperature}_{j,x} \times \text{ZOOP}_{j,x}$ $-U_1 \times \sigma_t \times \text{BACT} \times (\text{N/C bact}) + \alpha_{\text{bact}}\text{ON}_i \times \text{mbact}\ x_i \times \sigma_t\ \text{x BACT}^{1.65}$ $\times (\text{N/C bact}) - (Detritus\ N_x/ON_x \times Vbiosettling + (1\text{-}Detritus\ N_x/ON_x) \times Vsettling) \times ON_x/z_x - KNmineral_x \times ON_x + ONEXOG_x + ONENDO_x - Outflows \times ON$
	Biogenic organic nitrogen accumulation	$Detritus\ N_x$	$= \sum_i (1 - aNH4_i) \times mp_i \times e^{kt(Tx\text{-}Tempref)} \times N/C_{i,x} \times PHYT_{i,x} + (1 - aNH4_{zoo}) \times mz \times e^{kt(Tx\text{-}Tempref)} \times N/C_{zoo} \times ZOOP_x$
	Loss due to zooplankton grazing upon detritus	$DetritusGrazingN$	$= maxgrazing \times Pref_{det\ x} \times Detritus\ N_x/(KZ + Food_x)$
	ON flux from sediment	$ONENDO_x$	$= TurbFish + \varepsilon ON + ONSED_x$
	Wind resuspension	εON	$= \alpha_0 \times ((\sigma - \sigma_c)/\sigma_c)^b\ if\ \sigma \ge \sigma_c,\ 0\ if\ \sigma < \sigma_c$
		$ONSED_x$	$= ONosed \times e^{(kt_{sed}(\text{Tsed-Tempref}_{sed})}$, where
	Rate of sediment release of organic nitrogen	$ONosed$	$= OPosed \times TN/TP,$
10	**Sediment submodel**		
10.1	**Phosphate sediment release**	$\frac{dPO_{4sed_x}}{dt}$	$= (1 - \beta_P) \times Pdeposition - (\alpha s_{PO4} \times PO4_{sed\ x} \times e^{Ktsed(Tsedx\text{-}Tempref sed)})$
	Organic phosphorus sedimentation	$Pdeposition$	$= (\sum_i Vsettling_i \times Pint_{i,x} \times PHYT_{i,x} + SettlingP_x \times OP_x)$
10.2	**Ammonium sediment release**	$\frac{dNH_{4sed_x}}{dt}$	$= (1 - \beta_N) \times Ndeposition$ $-(\alpha s_{NH4} \times NH4_{sed} \times e^{Ktsed\ (Tsed\ x\text{-}\ Tempref sed)})$ $- Nitrifmax_{sed} \times (DO_x/(DO_x + KHdonit_{sed})) \times$ $\times (NH_{4\ sed\ x}/(KHnh4nit_{sed} + NH_{4\ sed\ x})) \times ftempnitrsed_x$
	Loss due to particulate nitrogen settling	$Ndeposition$	$= \sum_i Vsettling_i \times N/C_{i,x} \times PHYT_{i,x} + SettlingN_x \times ON_x$
	Temperature limitation for nitrification in the sediments	$ftempnitrsed_x$	$= e^{(-KTgrnitr_{sed}(T_x\text{-}Toptnitr_{sed})^2)}$
10.3	**Nitrate sediment release**	$\frac{dNO_{3sed_x}}{dt}$	$= Nitrifmax_{sed} \times (DO_x/(DO_x + KHdonit)) \times (NH_{4sed\ x}/(KHnh4nit + NH_{4sed\ x})) \times ftempnitr_x - (as_{NO3} \times NO3_{sed\ x} \times e^{Ktsed(Tsedx\text{-}Tempref sed)}) - Denitrifmax_{sed} \times (KHdodenit_{sed}/(DO_x + KHdodenit_{sed})) \times (NO_{3sed\ x}/KHno3denit_{sed} + NO_{3\ sed\ x}) \times ftempdenitrsed_x$
	Temperature limitation for denitrification in the sediments	$ftempdenitrsed_x$	$= e^{(-KTgrdenitr_{sed}(T_x\text{-}Toptdenitr_{sed})^2)}$
	Rate of sediment release of organic nitrogen	$ONSED_x$	$= ONosed \times e^{(kt_{sed}(\text{Tsed-Tempref}_{sed})}$, where
		$ONosed$	$= OPosed \times TN/TP,$

i = phytoplankton functional group (cyanobacteria, non-cyanobacteria) ; x = vertical layer, x=1; j = zooplankton group, j = 1.

nutrient uptake depends on both intracellular and extracellular concentrations and it is restricted by upper and lower internal storage capacity bounds. Our model postulates a unimodal response with respect to the dependence of phytoplankton growth on temperature, which is modeled by a function similar to a Gaussian probability curve (Cerco and Cole, 1994). The photosynthesis and light intensity relationship is depicted by Steele's equation with Beer's law to scale photosynthetically active radiation to depth (Arhonditsis and Brett, 2005a). Based on multiple regression analysis performed with empirical data from the study period, we identified chlorophyll-a and SS as the main factors influencing the light availability in the lagoon. Consequently, the extinction coefficient (K_d) was determined as the sum of the background light attenuation (representing water absorption), the attenuation due to chlorophyll a, and total suspended solids (Jassby and Platt, 1976). The model-based and empirically-derived K_d values were found to be comparable (mean $5 \pm 0.6\ m^{-1}$ and $4.6 \pm 1.3\ m^{-1}$, respectively) supporting the validity of our estimations. Phytoplankton mortality includes natural mortality as well as all internal processes that reduce algal biomass (respiration, excretion) and is assumed to increase exponentially with temperature. Phytoplankton settling considers the loss of biomass caused by algal sinking to the bottom of the lagoon. Zooplankton grazing was parameterized as a function of the observed zooplankton biomass data using a Michaelis-Menten equation while accounting for temperature dependence. The equation considers different food sources which are grazed upon with preference that changes dynamically as a function of their relative proportion (Fasham et al., 1990). In terms of

Table 2
Definitions and calibration values of the model parameters.

Symbol	Description	Values	Units	Sources
α_0	Wind resuspension coefficient	0.008	mg m^{-2} day^{-1}	1
$\alpha_{DOC\ zoo}$	Fraction of zooplankton mortality becoming dissolved organic carbon	0.3		10
$\alpha_{DOC\ cyano}$	Fraction of cyanobacteria mortality becoming dissolved organic carbon	0.3	-	10
$\alpha_{DOC\ non\text{-}cy}$	Fraction of non-cyanobacteria mortality becoming dissolved organic carbon	0.3	-	10
$\alpha_{NH4\ zoo}$	Fraction of zooplankton mortality becoming ammonium	0.13	-	10
$\alpha_{NH4\ cyano}$	Fraction of cyanobacteria mortality becoming ammonium	0.13	-	10
$\alpha_{NH4\ non\text{-}cy}$	Fraction of non- cyanobacteria mortality becoming ammonium	0.13	-	10
$\alpha_{NH4\ BACT}$	Fraction of bacteria mortality becoming ammonium	0.13	-	10
$\alpha_{ON\ BACT}$	Fraction of bacteria mortality becoming organic nitrogen	0.85	-	10
$\alpha_{PO4\ zoo}$	Fraction of zooplankton mortality becoming phosphate	0.3	-	10
$\alpha_{PO4\ cyano}$	Fraction of cyanobacteria mortality becoming phosphate	0.3	-	10
$\alpha_{PO4\ non\text{-}cy}$	Fraction of non-cyanobacteria mortality becoming phosphate	0.3	-	10
αs_{NO3}	Sediment nitrate release rate	0.5	day^{-1}	-
αs_{NH4}	Sediment ammonium release rate	0.5	day^{-1}	-
αs_{PO4}	Sediment phosphate release rate	0.5	day^{-1}	-
$asfood_{\ det}$	Zooplankton assimilation efficiency for detritus	0.3	-	-
$asfood_{cyano}$	Zooplankton assimilation efficiency for cyanobacteria	0.25	-	-
$asfood_{\ non\text{-}cy}$	Zooplankton assimilation efficiency for non-cyanobacteria	0.5	-	-
$asfood_{BACT}$	Zooplankton assimilation efficiency for bacteria	0.45	-	-
b	Sediment bed shear stress exponent	3	-	20
$ChlaC_{\ cyano}$	Chlorophyll to carbon ratio in cyanobacteria	0.02	-	8,9,11,14
$ChlaC_{\ non\text{-}cy}$	Chlorophyll to carbon ratio in non- cyanobacteria	0.02	-	8,9,11,14
$Denitrifmax$	Maximum denitrification rate	20	mg N m^{-2} day^{-1}	-
$Denitrifmax_{sed}$	Maximum sediment denitrification rate	25	mg N m^{-2} day^{-1}	-
$gwthmax_{cyano}$	Maximum growth rate for cyanobacteria	0.9	day^{-1}	13,17,18
$gwthmax_{non\text{-}cy}$	Maximum growth rate for non-cyanobacteria	1.5	day^{-1}	13
Ik_{cyano}	Half saturation light intensity for cyanobacteria	150	MJ m^{-2} day^{-1}	-
$Ik_{non\text{-}cy}$	Half saturation light intensity for non-cyanobacteria	250	MJ m^{-2} day^{-1}	-
$KCrefmineral$	Particulate carbon mineralization rate at reference temperature	0.01	day^{-1}	-
$K_d b$	Background light attenuation	1.55	m^{-1}	-
$K_d chla$	Light attenuation coefficient for chlorophyll	0.014	m^2 mg^{-1}	-
$K_d SS$	Light attenuation coefficient for suspended solids	0.014	m^2 mg^{-1}	-
KB	Half saturation constant for bacterial uptake	200	mg N^{-1} day^{-1}	
$KHdodenit$	Half saturation concentration of DO deficit required for nitrification	0.5	mg O_2 m^{-3}	10
$KHdodenit_{sed}$	Half saturation concentration of DO deficit required for denitrification in the sediments	1	mg O_2 m^{-3}	-
$KHdonit$	Half saturation concentration of DO required for nitrification	1	mg O_2 m^{-3}	10
$KHdonit_{sed}$	Half saturation concentration of DO required for nitrification in the sediments	2	mg O_2 m^{-3}	-
$KHnh4nit$	Half saturation concentration of ammonium required for nitrification	1	mg N m^{-3}	10
$KHnh4nit_{sed}$	Half saturation concentration of ammonium required for nitrification in the sediments	75	mg N m^{-3}	-
$KHno3denit$	Half saturation concentration of nitrate required for denitrification	15000	mg N m^{-3}	21*
$KHno3denit_{sed}$	Half saturation concentration of DO deficit required for denitrification in the sediments	15	mg O_2 m^{-3}	-
KN_{cyano}	Half saturation constant for nitrogen uptake by cyanobacteria	125	mg N m^{-3}	-
$KN_{non\text{-}cy}$	Half saturation constant for nitrogen uptake by non-cyanobacteria	150	mg N m^{-3}	-
$KNrefmineral$	Nitrogen mineralization rate at reference temperature	0.01	day^{-1}	10,14
KP_{cyano}	Half saturation constant for phosphorus uptake by cyanobacteria	18	mg P m^{-3}	12
$KP_{non\text{-}cy}$	Half saturation constant for phosphorus uptake by non-cyanobacteria	13	mg P m^{-3}	21*
$KPrefmineral$	Phosphorus mineralization rate at reference temperature	0.005	day^{-1}	3,14,10
KT	Effects of temperature on phytoplankton mortality	0.05	$°C^{-1}$	3,7
$KTFmin$	Effects of temperature on mineralization	0.004	$°C^{-2}$	-
$KTgrdenitr$	Effect of temperature on denitrification	0.004	$°C^{-2}$	-
$KTgrdenitr_{sed}$	Effect of temperature on sediment denitrification	0.004	$°C^{-2}$	-
$KTgr1_{zoo}$	Effect of temperature on zooplankton	0.005	$°C^{-2}$	8,3
$KTgr2_{zoo}$	Effect of temperature on zooplankton	0.005	$°C^{-2}$	8,3
$KTgrnitr$	Effect of temperature on nitrification	0.004	$°C^{-2}$	10,15
$KTgrnitr_{sed}$	Effect of temperature on sediment nitrification	0.004	$°C^{-2}$	-
$KTgr_{cyano}$	Effect of temperature on cyanobacteria	0.005	$°C^{-2}$	3,10,12,13
$KTgr_{non\text{-}cy}$	Effect of temperature on non-cyanobacteria	0.005	$°C^{-2}$	3,10,12,13
kt_{sed}	Effects of temperature on sedimentation	0.004	-	-
KZ	Half saturation constant for grazing by zooplankton	105	mg C m^{-3}	6-7
$maxgrazing$	Maximum grazing rate for zooplankton	0.415	day^{-1}	6-7
mb	Mortality rate for bacteria	0.009	day^{-1}	22*
mp_{cyano}	Mortality rate for cyanobacteria	0.009	day^{-1}	7,14
$mp_{non\text{-}cy}$	Mortality rate for non-cyanobacteria	0.01	day^{-1}	7,10, 14
mz	Mortality rate for zooplankton	0.13	day^{-1}	19, 6,7, 8
N/C_{zoo}	Nitrogen to carbon ratio for zooplankton	0.2	mg N mg C^{-1}	2,16
N/C_{bact}	Nitrogen to carbon ratio for bacteria	0.18		
$Nitrifmax$	Maximum nitrification rate at optimal temperature	20	mg N m^{-3} day^{-1}	10,14,15
$Nitrifmax_{sed}$	Maximum sediment nitrification rate	50	mg N m^{-2} day^{-1}	10,15,19
$Nmax_{cyano}$	Maximum cyanobacteria internal nitrogen	0.4	mg P mg C^{-1}	7
$Nmax_{non\text{-}cy}$	Maximum non-cyanobacteria internal nitrogen	0.1	mg P mg C^{-1}	7
$Nmaxuptake_{cyano}$	Maximum nitrogen uptake rate for cyanobacteria	0.25	mg P mg C^{-1} day^{-1}	7, 14
$Nmaxuptake_{non\text{-}cy}$	Maximum nitrogen uptake rate for non-cyanobacteria	0.25	mg P mg C^{-1} day^{-1}	7, 14
$Nmin_{cyano}$	Minimum cyanobacteria internal nitrogen	0.3	mg P mg C^{-1}	7
$Nmin_{non\text{-}cy}$	Minimum non-cyanobacteria internal nitrogen	0.005	mg P mg C^{-1}	7, 14
P/C_{zoo}	Phosphorus to carbon ratio for herbivorous zooplankton	0.025	mg P mg C^{-1}	2,16

Table 2 (*continued*)

Symbol	Description	Values	Units	Sources
$Pmax_{cyano}$	Maximum cyanobacteria internal phosphate	0.004	mg P mg C^{-1}	7
$Pmax_{non\text{-}cy}$	Maximum non-cyanobacteria internal phosphate	0.019	mg P mg C^{-1}	7, 14
$Pmaxuptake_{cyano}$	Maximum phosphorus uptake rate for cyanobacteria	0.03	mg P mg C^{-1} day^{-1}	7
$Pmaxuptake_{non\text{-}cy}$	Maximum phosphorus uptake rate for non-cyanobacteria	0.025	mg P mg C^{-1} day^{-1}	7
$Pmin_{cyano}$	Minimum cyanobacteria internal phosphorus	0.001	mg P mg C^{-1}	7
$Pmin_{non\text{-}cy}$	Minimum non-cyanobacteria internal phosphorus	0.001	mg P mg C^{-1}	7
Pred	Fish predation constant	400	mg C m^{-3}	-
$Pref_{det}$	Preference of zooplankton for detritus	0.5	-	-
$Pref_{cyano}$	Preference of zooplankton for cyanobacteria	0.25	-	-
$Pref_{non\text{-}cy}$	Preference of zooplankton for non-cyanobacteria	0.5	-	-
$Pref_{BACT}$	Preference of zooplankton for bacteria	0.5	-	-
Tempref	Water reference temperature	20	°C	3,7,10,11
$Tempref_{sed}$	Sediment reference temperature	20	°C	-
Toptdenitr	Optimal temperature for denitrification	20	°C	-
$Toptdenitr_{sed}$	Optimal temperature for denitrification in sediment	20	°C	-
$Tref_{fish}$	Reference temperature for bish bioturbation	25	°C	-
$Tref_{zoo}$	Reference temperature for zooplankton	20	°C	19,3-5,8
Toptmin	Optimal temperature for mineralization	20	°C	-
Toptnitr	Optimal temperature for nitrification	20	°C	10,15
$Toptnitr_{sed}$	Optimal temperature for denitrification in sediment	20	°C	-
$Tref_{cyano}$	Reference temperature for cyanobacteria metabolism	25	°C	21*
$Tref_{non\text{-}cy}$	Reference temperature for non-cyanobacteria	16.5	°C	21*
$uptakemax_{bact}$	Maximum bacterial uptake rate	1.6	day^{-1}	21*
$Vsettling_{(biogenic)}$	Biogenic particle settling velocity	0.025	m day^{-1}	-
Vsettling	Allochthonous particle settling velocity	0.025	m day^{-1}	21*
$Vsettling_{cyano}$	Cyanobacteria settling velocity	0.03	m day^{-1}	8
$Vsettling_{non\text{-}cy}$	Non-cyanobacteria settling velocity	0.05	m day^{-1}	8
β_N	Fraction of inert nitrogen buried into deeper sediment	0.9	-	-
β_P	Fraction of inert phosphorus buried into deeper sediment	0.9	-	-
	Shape parameter for the trigonometric functions $\sigma_{(t)}$ *and* $\sigma_{(tz)}$	0.5	-	-
σ	Sediment bed shear stress	-	N m^{-2}	20
σ_c	Critical sediment bed shear stress	0.07	N m^{-2}	-
v	Ratio of bacterial ammonium to DON uptake	0.75	-	22*

1) Mian and Yanful, 2004 2) Sterner et al., 1992; 3) Omlin et al., 2001; 4) Orcutt and Porter, 1983; 5) Downing and Rigler, 1984; 6) Sommer, 1989; 7) Jorgensen et al., 1991; 8) Wetzel, 2001; 9) Chen et al., 2002(and references therein); 10) Cerco and Cole, 1994 (and references therein); 11) Reynolds, 1984; 12) Arhonditsis and Brett, 2005a, 2005b; 13) Reynolds, 2006; 14) Hamilton and Schladow, 1997 (and references therein); 15) Berounsky and Nixon, 1990; 16) Hessen and Lyche, 1991; 17) Romo and Miracle, 1993; 18) Romo, 1994; 19) Lampert et al., 1997; 20) Chao et al., 2008; 21) Gudimov et al., 2010; 22) Arhonditsis et al., 2008.
* Subject to calibration.

their palatability, our model assumes that zooplankton prioritizes the ingestion of non-cyanobacteria, detritus, and heterotrophic bacteria over cyanobacteria.

2.2.2.2. Bacteria. Detailed information on heterotrophic bacterial biomass and production in Albufera de Valencia can be found in a recent study by Onandia et al., 2014a. Bacterial biomass varies significantly among seasons and was remarkably high (1 — 3.6 mg C L^{-1}), surpassing similar measurements in highly eutrophic lakes. Bacterial production showed minor seasonal variations, varying between 186 — 390 mg C $m^{-2}d^{-1}$ (Onandia et al., 2014a). The main terms included in the bacterial biomass equation are growth and losses due to zooplankton grazing, mortality, and outflows. Bacterial growth follows the mathematical representation proposed by Fasham et al. (1990) and depends on dissolved organic nitrogen (DON) and ammonium availability. To ensure that bacterial biomass is produced with a constant ratio of bacterial ammonium to DON uptake, a total nitrogenous substrate S is considered. A quadratic function was used to model the loss of bacterial biomass due to mortality and excretion (Arhonditsis et al., 2008). This formulation corresponds to a loss rate dependent on the bacterial biomass itself and (aside from the metabolic losses) may be interpreted as representing bacterivory by other consumers (e.g., heterotrophic nanoflagellates, mixotrophic flagellates, ciliates) whose biomass is proportional to that of bacteria.

2.2.2.3. Phosphorus. The model considers two phosphorus state variables: phosphate (PO_4) and organic phosphorus (OP). The phosphate equation considers phytoplankton uptake, the fraction of phytoplankton and zooplankton mortality that is directly supplied into the system in inorganic form, and the bacteria-mediated mineralization of organic phosphorus. The organic phosphorus equation considers the fraction of organic phosphorus that is returned into the system via mortality of both phytoplankton and zooplankton. Part of the organic phosphorus settles to the sediment and another fraction is mineralized into phosphate. External phosphorus loads in the system via atmospheric deposition and terrestrial loadings as well as losses via the outflows into the Mediterranean Sea are also taken into account.

2.2.2.4. Nitrogen. There are three nitrogen forms considered by the model: ammonia, nitrate and organic nitrogen. The ammonia equation considers phytoplankton and bacteria uptake as well as the fraction of phytoplankton, bacteria and zooplankton mortality that is released into the water column. In a well-oxygenated water column, ammonia is oxidized to nitrate through nitrification. The kinetics of this reaction is modeled as a function of ammonia, dissolved oxygen, temperature, and light availability in the system (Cerco and Cole, 1994; Tian et al., 2001). The mineralization of organic nitrogen to ammonium is also taken into account. The nitrate equation considers uptake by phytoplankton. The ammonium inhibition of nitrate uptake is based on the relative abundance of the two inorganic nitrogen forms. Ammonia is oxidized to nitrate through nitrification and conversely, nitrate is lost through denitrification as nitrogen in the gaseous from. Denitrification is modeled as a function of nitrate, dissolved oxygen and temperature availability (Arhonditsis and Brett, 2005a). The organic nitrogen equation considers the inputs through phytoplankton, zooplankton, and bacteria basal metabolism. The losses stem from detritus grazing and bacteria uptake. A fraction of organic nitrogen settles to the sediment and another fraction is mineralized by bacteria to ammonium. External inflows into the system as well as losses via outflows are also considered.

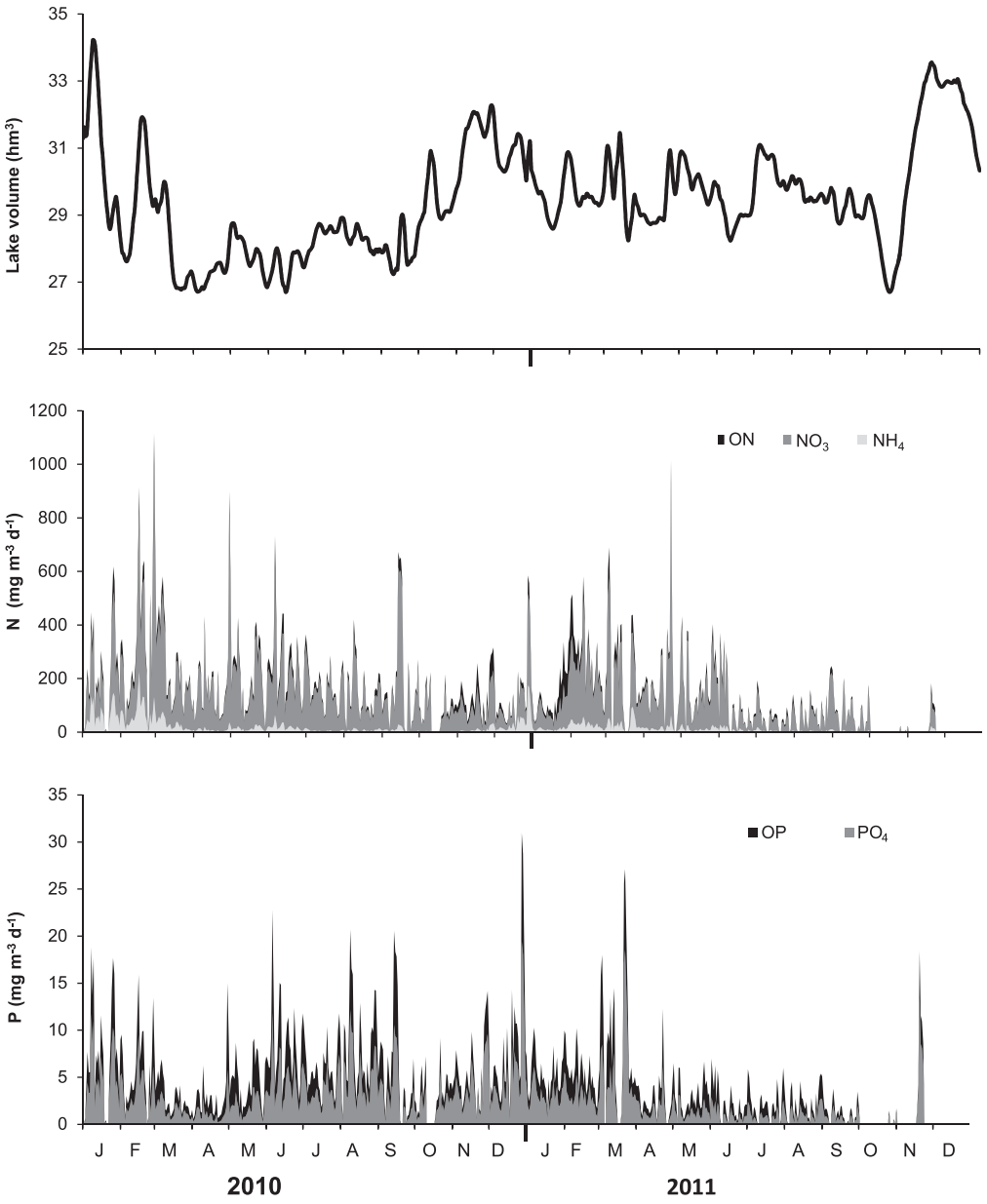

Fig. 2. Lagoon volume (upper panel), terrestrial nitrogen and phosphorus loadings (N and P, middle and lower panels) during the study period.

2.2.2.5. Fluxes from the sediment. Because the existing empirical information was not adequate to develop a process-based sediment diagenesis submodel, the interactions between sediment and water column were depicted following a simple dynamic approach that links the temperature-dependent nitrogen and phosphorus fluxes from the sediment with sedimentation (algal and particulate matter) and burial rates (Arhonditsis and Brett, 2005a). The relative magnitude of ammonium and nitrate fluxes was also determined by nitrification occurring at the sediment surface. The influence of wind resuspension and fish bioturbation on the P and N organic fractions accumulated onto the sediment top layers were also taken into account. Similar to Kim et al. (2013), we used an empirical expression that postulates a linear relationship between sediment resuspension rate and the excess bed shear stress (Chao et al., 2008; Mehta and Partheniades, 1982). The shear stress was calculated as a function of the wave characteristics (height, period length), water depth, wind speed, and fetch length using the equations introduced by Sverdrup-Munk-Bretschneider for shallow water bodies (Ijima and Tang, 1966). Data on nutrient concentrations in the sediments were based on previous measurements in the lake (Monerris, 1998). Regarding the impact of fish bioturbation, we used a linear relationship to depict the fact that resuspension caused by benthivorous fish during food search increases linearly with their corresponding biomass (Breukelaar et al., 1994). A correction for temperature was also applied, assuming a unimodal response pattern. Fish bioturbation estimates were based on the mean annual fish production in the lagoon for the period 1980-2002, as provided by Comunidad de Pescadores del Palmar (Blanco and Romo, 2006).

2.3. Model calibration/validation-Sensitivity analysis

The model was calibrated to match the observed patterns in the lagoon during the first year (2010) of the study by adjusting manually the model parameters within the ranges reported in the literature. The calibration vector which yielded the best fit between predicted and

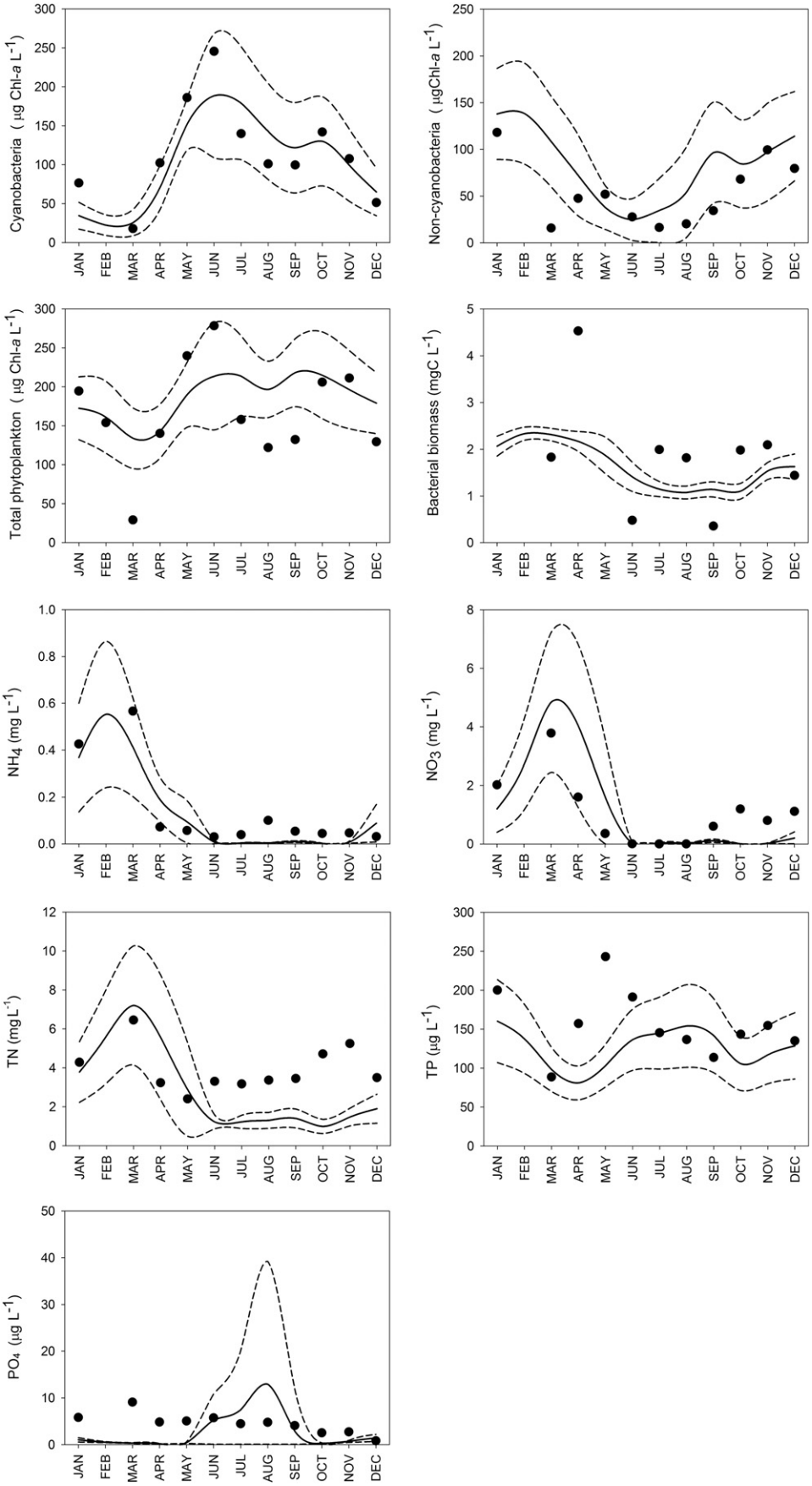

Fig. 3. Comparison between the monthly observed values and model predictions for phytoplankton, cyanobacteria, non-cyanobacteria, NH_4, NO_3, TN, PO_4, TP and bacteria during the calibration period (2010). Black dots represent the observed data and solid lines represent the model predictions, while dotted lines represent the 95% uncertainty bounds associated with the external forcing of the model.

observed data is shown in Table 2. Subsequently, we used observed data from 2011 to validate the model and evaluate its capacity to predict the ecosystem response under external conditions (somewhat) different from those used during the calibration. The model performance during the calibration and validation periods was evaluated by calculating two goodness-of-fit statistics: relative error (RE) and modeling efficiency (ME). The relative error is a scale-independent metric, reflecting the percentage discrepancy between predicted and observed values. The modeling efficiency assesses the predictive ability of the model using as a reference level the observed average values. A modeling efficiency close to one indicates that the model accurately fits the observations, whereas a value near zero indicates that model predictions for individual observations are as efficient as the observed average, while values below zero indicate that the average of the observed data would be a better predictor than the model itself (Stow et al., 2003).

A relative sensitivity measure was applied to identify the most influential model parameters for the predicted chlorophyll *a* values. All model parameters (with the exception of $ChlaC_{cyano}$, $ChlaC_{non\text{-}cy}$, KB, K_dchla, K_db, K_dSS, mz, N/C_{zoo}, P/C_{zoo}, ε, ψ, ν, $KHdonit_{sed}$, $KHnh4nit_{sed}$, $KHno3denit_{sed}$, $KHdodenit_{sed}$, $OPosed$) were increased and decreased by 10%, 20% and 50% and the effect on phytoplankton (total chlorophyll *a*), cyanobacteria and non-cyanobacteria daily values was expressed by their relative sensitivity (RS_i), as described in Zhang and Rao (2012):

$$RS_i = \frac{\Delta Y_i / Y_i}{\Delta\theta/\theta}$$

where Y_i is the daily value of the state variable after the model calibration, ΔY_i represents the change in the modeled value, θ is the parameter value assigned after the model calibration, and $\Delta\theta$ denotes the corresponding parameter perturbation. Based on all RS_i daily values, we subsequently calculated the mean annual relative sensitivity ($\overline{RS}$).

In addition, we attempted to quantify the impact of the uncertainty associated with the model forcing functions on the predictive statements drawn by the model. We introduced independent perturbations to N and P loading, outflows, zooplankton biomass, N and P burial rates, and subsequently quantified the changes of the predicted state variables. More specifically, we used Latin Hypercube sampling to obtain 1000 input vectors from the uncertainty zone of the forcing functions. These vectors were used to run the model and generate matrices (1000 x 12) that contained the average monthly values for phytoplankton, cyanobacteria, non-cyanobacteria, total phosphorus, phosphate, total nitrogen, nitrate, ammonium, and bacteria. According to the Ecoframe scheme proposed by Moss et al. (2003), the system must achieve a good ecological status through the implementation of suitable restoration actions. Since the reduction of nutrient inputs alone seems to be insufficient, the combination with other remedial measures might be required. In a system where the hydrological cycle is tightly linked to the seasonal succession of phytoplankton, the modulation of the flushing rate represents another potentially effective management strategy. We simulated a total of 72 combinations of N and P inflow concentrations, ranging from 50 to 130 % of the mean annual values recorded in 2010 (or flow-weighted mean concentrations ranging from 4.4 to 11.3 mg TN L^{-1} and from 130 to 340 μg TP L^{-1}, respectively), against flushing rates, ranging from 75% to 135% of the mean annual renewal in 2010 (or 6.7 to 13 y^{-1}). [It should be noted that the variations of the input nutrient concentrations corresponded to inflowing loadings of 2.8 to 7.2 x 10^3 kg N y^{-1} and 0.08 to 0.22 x 10^3 kg P y^{-1}, respectively.] These scenarios aimed to explore the potential response of the lagoon to a wide range of hydraulic and nutrient loading regimes.

3. Results

3.1. Model predictions and observed lake dynamics

The comparison between simulated and observed values along with the 95% uncertainty bounds during the first survey year (2010) are shown in Fig. 3. Generally, the model realistically reproduces the observed seasonal cycle of the two phytoplankton groups. The simulated total phytoplankton biomass is in reasonable agreement with the measured chlorophyll *a* concentrations. Nonetheless, the model cannot fully reproduce the so-called clear-water phase in March 2010, although there was a distinct wane in the simulated phytoplankton patterns. Likewise, the predicted annual cycle of the functional group labeled as "non-cyanobacteria" agrees with the observed data, aside from the late winter/early spring values (February-March) when the model fails to capture the sharp decrease and subsequent rebounding of the phytoplankton biomass. The model accurately replicates the average monthly cyanobacteria biomass levels along with the corresponding minimum (≈20 μg chl*a* L^{-1}) and maximum (≈250 μg chl*a* L^{-1}) values included in our calibration dataset. The model is capable of reproducing the average bacterial biomass levels in the lagoon, although the simulated bacteria displayed a static behaviour when compared to the moderately dynamic pattern observed. Nitrate predictions closely followed the observed annual cycle. However, the observed nitrate values in the fall (≈600-1200 μg L^{-1}) are underestimated by the model (≈10-200 μg L^{-1}). The seasonal variability of the ammonium concentrations is accurately predicted by the model, including the spring maximum levels (≈550 μg L^{-1}). Likewise, the predicted total nitrogen concentrations follow the measured values during the spring peak, but the model clearly underpredicts the observed patterns during the summer and fall period. Similar underestimation was found with the phosphate levels, although the summer concentrations were within the uncertainty bounds. Finally, aside from the underestimated spring peak (≈250 μg L^{-1}), the total phosphorus dynamics are fairly well simulated by our model.

Fig. 4 illustrates the comparison between predicted and observed values, along with the 95% uncertainty bounds, during the second survey year (2011). As previously noted, no clear-water phase occurred in the validation domain of our model. The minimum total phytoplankton values were recorded in March 2011, around 80 μg chl*a* L^{-1}. The same trend is also reproduced by the model, although the model significantly underestimates both the main spring peak and the secondary phytoplankton biomass increase recorded in the fall. This underestimation reflects the predictive error associated with the cyanobacteria simulations. By contrast, the model predictions overstate the observed non-cyanobacteria levels. In spite of these discrepancies, the model successfully captures the observed seasonal trends for both phytoplankton groups. Similar to the calibration results, the average bacterial biomass values are reasonably reproduced, although the model fails to mimic their seasonal variability. Regarding the nitrogen dynamics, nitrate predictions closely follow the observed annual cycle, but the simulated values underestimate the observed monthly levels from September to December. The seasonal ammonium pattern is reasonably predicted, with an overprediction problem from January to June. Similar to the calibration results, phosphate is underestimated for most of the annual cycle, whereas total phosphorus dynamics are fairly well reproduced by the model.

The relative error values derived from our calibration exercise suggest that among all the state variables, total phytoplankton (27%), cyanobacteria (24%), and total phosphorus (26%) showed the smallest discrepancy between measured values and model predictions, whereas phosphate displayed the highest relative error, 81% (Table 3). The maximum modeling efficiency was found for cyanobacteria and ammonium, with values greater than 0.70, whereas negative values were obtained for non-cyanobacteria, phosphate, total nitrogen, and total phosphorus. During the validation period, total phytoplankton and total phosphorus

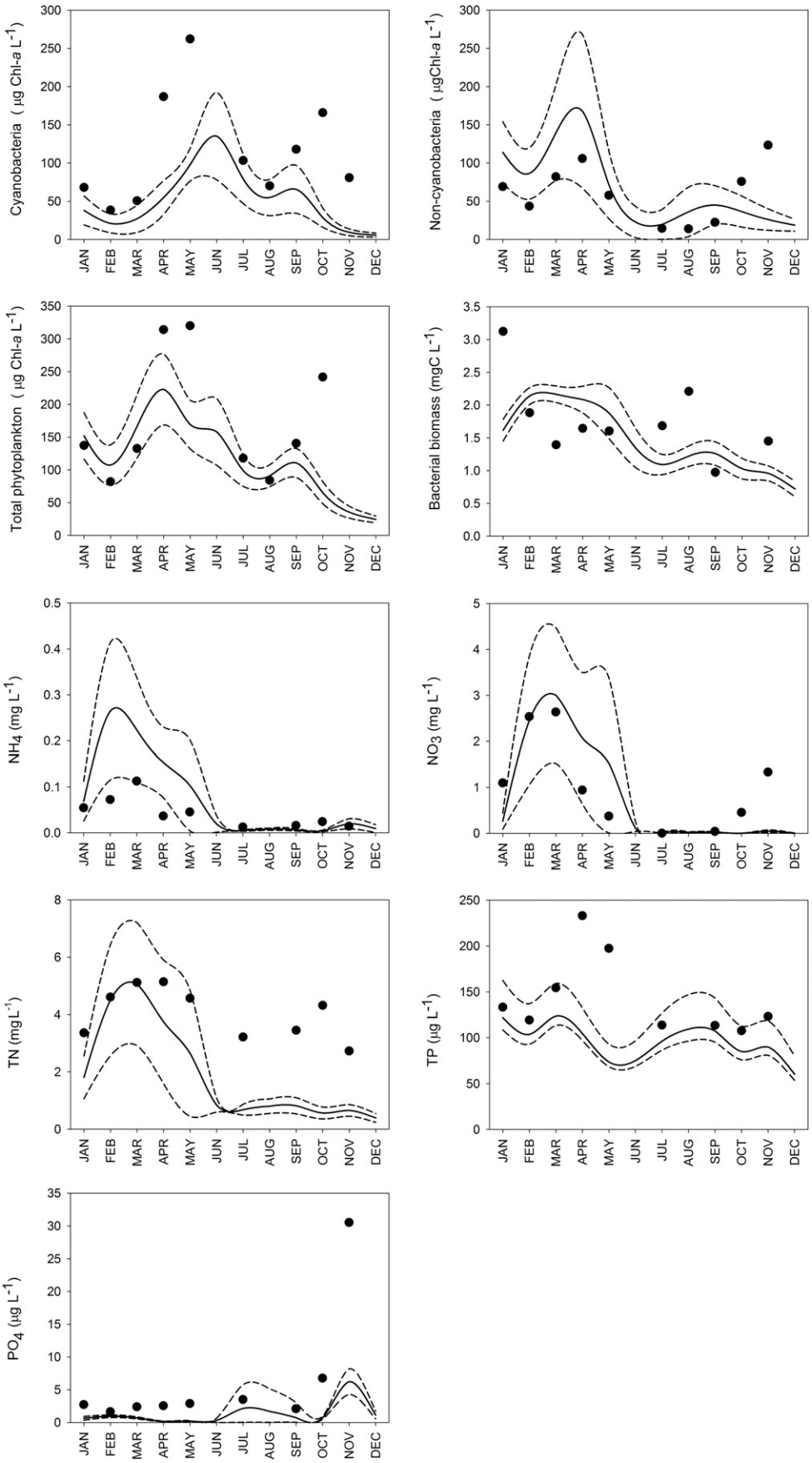

Fig. 4. Comparison between the monthly observed values and model predictions for phytoplankton, cyanobacteria, non-cyanobacteria, NH_4, NO_3, TN, PO_4, TP and bacteria during the validation period (2011). Black dots represent the observed data and solid lines represent the model predictions, while dotted lines represent the 95% uncertainty bounds associated with the external forcing of the model.

Table 3
Goodness-of-fit statistics for model outputs during the calibration and validation periods.

State variables	2010		2011	
	MEF	RE	MEF	RE
Bacteria (mg C L^{-1})	0.16	0.47	0.34	0.54
Phytoplankton chl *a* (μg L^{-1})	0.20	0.27	-0.34	0.40
Cyanobacteria chl *a* (μg L^{-1})	0.71	0.24	-0.64	0.58
Non-cyanobacteria chl *a* (μg L-1)	-0.37	0.56	-0.81	0.67
Ammonium (mg L^{-1})	0.82	0.48	-6.70	1.38
Nitrate (mg L^{-1})	0.02	0.78	0.31	0.57
Phosphate (μg L^{-1})	-4.03	0.81	0.05	0.77
Total nitrogen (mg L^{-1})	-3.03	0.49	-5.35	0.44
Total phosphorus (μg L^{-1})	-0.87	0.26	-1.31	0.30

Model Efficiency: $ME = \frac{\sum (Y_{OBSi} - \overline{Y})^2 - \sum (Y_{PREDi} - Y_{OBSi})^2}{\sum (Y_{OBSi} - \overline{Y})^2}$.

Relative Error: $RE = \frac{\sum |Y_{OBSi} - Y_{PREDi}|}{\sum Y_{OBSi}}$.

showed the lowest relative error values (<40%), but cyanobacteria error (58%) increased markedly comparing with the value obtained from the calibration exercise. Both phosphate and ammonium presented the highest discrepancies between model predictions and observations in 2011 (Table 3). In regard to the modeling efficiency, phosphate, nitrate and bacteria were characterized by positive values. However, the rest of the state variables had a negative modeling efficiency, suggesting that the predictive ability of the model has not been proven yet. In particular, the highest relative error and lower modeling efficiency in the validation domain may be indicative of a model overfitting; that is, an evidence of a series of parameter misspecifications during the model training that canceled each other out providing higher model performance with the calibration dataset.

3.2. Nitrogen and phosphorus budgets

The simulated annual nitrogen and phosphorus cycles, depicting the exogenous nutrient loadings and fluxes of the ecological processes considered are displayed in Fig. 5A,B. As previously mentioned, the external loading was based on flow-weighted nutrient concentrations measured in the channels throughout the study period 2010-2011. The model considers a hydrological annual loading of 231 hm^3 y^{-1} from fluvial and aerial sources. Taking into account the losses due to evaporation at the lagoon surface, the hydrological inputs result in a flushing rate of 8.9 y^{-1}. Terrestrial and atmospheric total nitrogen loadings, mainly in the form of nitrate, add 2209 x 10^3 kg N y^{-1} into the system and only a small fraction of 520 x 10^3 kg N y^{-1} (24%) is lost from the lagoon through the outlet channels, resulting in a net loading of 1689 x 10^3 kg N y^{-1}. Regarding the phosphorus budget, the net inputs in the system are 45.8 x 10^3 kg P y^{-1}. Terrestrial and atmospheric inputs are 65.5 x 10^3 kg P y^{-1}, 30% of which (19.7 x 10^3 kg P y^{-1}) flow out of the lagoon. Net phytoplankton growth (uptake minus basal metabolism) utilizes 1591 x 10^3 kg y^{-1} of nitrogen and 42 x 10^3 kg y^{-1} of phosphorus. Cyanobacteria net growth removes more than 80% of the nitrogen pool; namely, 1298 x 10^3 kg y^{-1}. On the other hand, non-cyanobacteria utilize 30.3 x 10^3 kg y^{-1} of phosphorus, which represents more than 70% of the phosphorus removal by phytoplankton. Bacteria mediated mineralization combined with plankton basal metabolism contribute 3.9 x 10^3 kg P y^{-1}, suggesting that the phytoplankton phosphorus requirements (47 x 10^3 kg P y^{-1}) cannot be entirely met by nutrient recycling. Likewise, the total phytoplankton nitrogen demand (4434 x 10^3 kg y^{-1}) cannot be fully satisfied by nitrogen recycling (which adds to 2793 x 10^3 kg y^{-1}), although it is worth noting that the nitrogen excreted by bacteria basal metabolism alone would be sufficient to provide roughly half of the nitrogen required. Interestingly, our model suggests that the sediments (on average) act as a phosphorus sink at the annual scale. Whereas the amount of phosphorus that settles onto the sediments is 17 x 10^3 kg y^{-1}, 6.2 x 10^3 kg y^{-1} are released back into the water column, mainly in the form of phosphate. By contrast, our model suggests a net release of nitrogen from the sediments into the water column; that is, 154 x 10^3 kg y^{-1} of nitrogen are deposited on the sediments and 160 x 10^3 kg y^{-1} return into the water column, mostly as organic nitrogen.

3.3. Sensitivity analysis

Our sensitivity analysis examined the role of eighty eight (88) parameters. The twelve parameters with the highest relative sensitivity values with respect to the total phytoplankton and cyanobacteria predictions are shown in Table 4. Generally, the total phytoplankton and cyanobacteria have low $\overline{RS}$ values, although cyanobacteria demonstrated greater degree of sensitivity to the parameter perturbations induced. The parameters with a greatest influence on total phytoplankton and cyanobacteria biomass were those influencing phytoplankton growth and losses, such as maximum growth ($grthmax_{cyano}$, $grthmax_{non\text{-}cyano}$) and settling ($Vsettling_{cyano}$, $Vsettling_{non\text{-}cyano}$) rates of both phytoplankton groups. Other relevant factors were temperature-related parameters, such as water reference temperature ($Temp_{ref}$), reference temperature for zooplankton ($Tref_{zoo}$), reference temperature for cyanobacteria and non-cyanobacteria metabolism ($Tref_{cyano}$, $Tref_{non\text{-}cyano}$), and the effect of temperature on cyanobacteria growth ($KTgr_{cyano}$). Importantly, the degree of nutrient accumulation in the sediment compartment, as determined by the proportion of inert nitrogen and phosphorus buried into deeper sediment (β_N, β_P) represent a critical step of the system characterization. It is also interesting to note that the maximum quotas for phosphorus in non-cyanobacteria ($Pmax_{non\text{-}cyano}$) and nitrogen in cyanobacteria ($Nmax_{cyano}$) were also influential.

The parameter values of the calibration vector along with the tested perturbations (±10, 20 and 50% change) against the corresponding model outputs for mean annual total, cyanobacteria and non-cyanobacteria chlorophyll *a* concentrations are shown in Fig. 6. These plots illustrate the importance of the processes that shape the dynamics of the two phytoplankton groups as well as their competition patterns in our simulations. Maximum growth rates play a major role in the characterization of the competition between the two phytoplankton groups. The increase in the maximum growth rate for cyanobacteria ($gwthmax_{cyano}$) renders them a competitive advantage over the non-cyanobacteria, resulting in a decline of the latter functional group and smaller relative contribution to the total phytoplankton biomass. The opposite pattern holds true when the maximum growth rate for non-cyanobacteria ($gwthmax_{non\text{-}cyano}$) increases. However, a minimum increase of 20% in $gwthmax_{non\text{-}cyano}$ would be necessary for non-cyanobacteria to become the predominant group in the simulated algal assemblage. The settling rates assigned to the two functional groups affect in a similar manner their interactions. Our sensitivity analysis also identified the burial rates as a critical factor in shaping phytoplankton dynamics. For example, an increase in the fraction of inert nitrogen (β_N) and phosphorus (β_p) buried into deeper sediment would reduce the advantage of cyanobacteria and non-cyanobacteria in regards to the competition for the corresponding nutrients. Notably, our results also show that the specification of the reference temperature for cyanobacteria metabolism ($Tref_{cyano}$) affects the relative contribution of the two modeled groups to the total phytoplankton biomass. The model outputs were also sensitive to the fraction of bacteria mortality becoming organic nitrogen (α_{ONBACT}) in that an increase in the value assigned to this parameter would favor cyanobacteria dominance. Interestingly, the parameters associated with the cyanobacteria intracellular storage capacities ($Nmax_{cyano}$, $Nmin_{cyano}$,$Pmax_{cyano}$, $Pmin_{cyano}$), especially those related to P, were found to have fairly minimal impact in the interactions between the two phytoplankton functional groups. Similar results were found for the effect of temperature on cyanobacteria growth ($KTgr_{cyano}$).

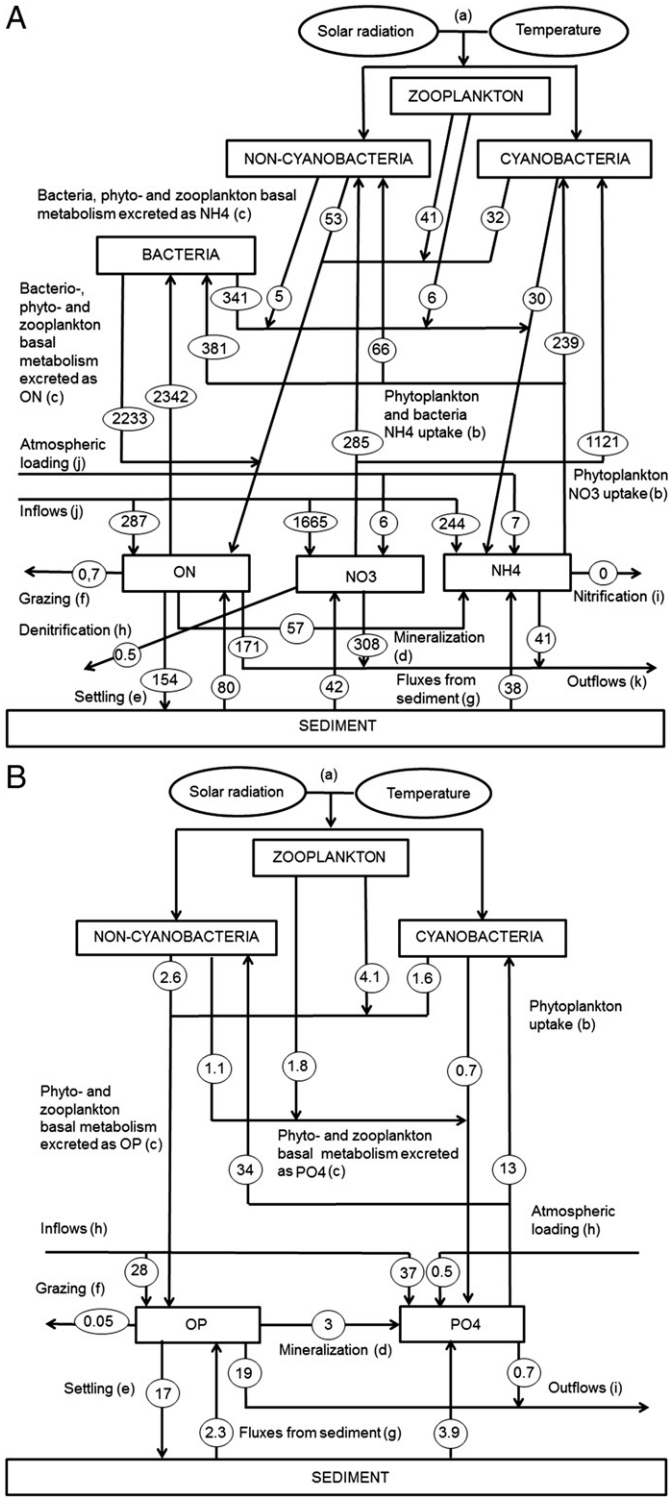

Fig. 5. (***A***) Nitrogen cycle: (a) external forcing to phytoplankton growth (temperature, solar radiation); (b) phytoplankton uptake; (c) bacterial, phytoplankton, and zooplankton basal metabolism excreted as NH_4 and ON; (d) ON mineralization; (e) particles settling; (f) detritus grazing; (g) NH_4, NO_3 and ON fluxes from sediment driven by diffusion, wind resuspension and fish bioturbation; (h) NO_3 losses due to denitrification (i) nitrification; (j) exogenous NH_4, NO_3 and ON inflows; (k) NH_4, NO_3 and ON outflows. (***B***) Phosphorus cycle: (a) external forcing to phytoplankton growth (temperature, solar radiation); (b) phytoplankton uptake; (c) bacteria, phytoplankton, and zooplankton basal metabolism excreted as PO_4 and OP; (d) OP mineralization; (e) particles settling; (f) detritus grazing; (g) PO_4, and OP fluxes from sediment driven by diffusion, wind resuspension and fish bioturbation; (h) exogenous NH_4, NO_3 and ON inflows; (i) NH_4, NO_3 and ON outflows. Given numbers represent cumulative annual N and P fluxes (t^{-1}).

3.4. Analysis of management scenarios

The model was subsequently used to examine the effects of alternative nutrient loading and hydraulic regimes on the phytoplankton mean annual levels, although we caution that its moderate capacity to reproduce the observed patterns could be an impediment to impartially infer the relative efficiency of different management practices in the lagoon. Because the variations in the flushing rates encompass a proportional nutrient loading change (e.g., increased flushing rates are accompanied by increased loading rates), the actual effects cannot be quantified unless we consider the concept of net loading. The net loading is simply calculated by multiplying the inflows from the exogenous sources with the difference in the nutrient concentrations between inflows and receiving water body, and thus weighs the different displacement of nutrients and phytoplankton biomass due to the variability in the corresponding flow regime induced (Kim et al., 2013). Hence, we accommodate the idea that two equal total loads with opposite pairs of flow and nutrient concentration, high flow with low concentration or low flow with high concentration, could potentially have different effects on the trophic state of the lagoon.

Our model projections suggest that both total annual phytoplankton and cyanobacteria biomass respond in a linear fashion to the variations of the nutrient loadings and flushing rates (Fig. 7; upper panels). The nutrient concentrations of the inflowing waters appear to exert greater control relative to the flushing rate, as depicted by the corresponding steeper gradients of the surface representing the predicted phytoplankton response. Importantly, the positive relationship between phytoplankton biomass and flushing rates suggests that the nutrient concentrations of the inflowing waters remain higher than the ambient levels, and thus the net loading into the system is positive within the range of hydraulic and exogenous nutrient levels examined (Fig. 8). Simply put, net increase of the ambient nutrient levels results even with a fast water renewal, which cannot be compensated by the advective transport of the particulate material (including algal cells) out of the lagoon. The most drastic reduction of the total phytoplankton biomass was achieved with a 50% reduction of TN and TP concentrations (4.4 mg TN L^{-1} and 130 μg TP L^{-1} or loading of 2.8 x 10^{-3} kg N day^{-1} and 0.08 x10^{-3} kg P day^{-1}, respectively) combined with a 25% decrease of the flushing rate (≈6.7 yr^{-1}), which resulted in an annual average of 91 μg chl*a* L^{-1}. Importantly, the latter projected value is approximately half of the model predictions (≈187 μg chl*a* L^{-1}) when forced with the current hydraulic and nutrient loading conditions. Under the same scenario, the cyanobacteria abundance biomass was reduced down to 47 μg chl*a* L^{-1} relative to the current model predictions of 104 μg chl*a* L^{-1}.

Finally, we note that the presented results refer to the average annual levels, and thus do not necessarily reflect the prevailing conditions in shorter time windows when the dilution effects of a higher flushing rate may actually be experienced. For example, when focusing on the February-March period, we can infer that the variability in the hydraulic regime can differentially impact the qualitative and quantitative features of the algal assemblage (Fig. 7; lower panels). In particular, while total annual phytoplankton and non-cyanobacteria biomass correspondingly demonstrate a marginal and moderate increase when faster flushing rates prevail, cyanobacteria display a distinctly declining trend, reflecting the fact that the biomass losses due to the elevated advective transport out of the lagoon cannot be counterbalanced by the slow growth rates assigned to the latter functional group.

4. Discussion

Elucidating the (often contrasting) phytoplankton patterns and understanding the underlying cause-effect relationships require rigorous quantitative tools with the ability to analyze multiple (direct and indirect) ecological pathways. The present study opted for the development of a mechanistic model to advance our understanding of the eutrophication processes in the shallow system of Albufera de Valencia and

Table 4
Sensitivity analysis of the Albufera de Valencia biogeochemical model. The twelve most influential parameters on chlorophyll *a* predictions, based on the relative sensitivity (RS) values. ± 10, 20 and 50% indicate percentage change applied to the parameter values assigned after model calibration.

Total chl *a*											
50%	RS	20%	RS	10%	RS	-50%	RS	-20%	RS	-10%	RS
$\alpha_{ON\ BACT}$	0.29	$\alpha_{ON\ BACT}$	0.32	$grthmax_{non\text{-}cy}$	0.31	$Nmax_{cyano}$	1.11	$grthmax_{non\text{-}cy}$	0.35	$grthmax_{non\text{-}cy}$	0.36
$grthmax_{non\text{-}cy}$	0.27	$grthmax_{non\text{-}cy}$	0.29	$\alpha_{ON\ BACT}$	0.25	$grthmax_{non\text{-}cy}$	0.45	$grthmax_{cyano}$	0.29	$Tref_{non\text{-}cy}$	0.18
$grthmax_{cyano}$	0.19	$grthmax_{cyano}$	0.21	$grthmax_{cy}$	0.22	$grthmax_{cyano}$	0.43	$Tref_{non\text{-}cy}$	0.20	$grthmax_{cyano}$	0.17
$Tref_{zoo}$	0.13	$Tref_{zoo}$	0.11	$Tref_{zoo}$	0.10	$Tref_{non\text{-}cy}$	0.21	$\alpha_{ON\ BACT}$	0.12	$\alpha_{ON\ BACT}$	0.14
Tempref	0.07	Tempref	0.08	Tempref	0.09	Tempref	0.11	Tempref	0.09	$Tref_{zoo}$	0.08
$Uptakemax_{bact}$	0.05	$Uptakemax_{bact}$	0.06	$Tref_{non\text{-}cy}$	0.07	$Pmaxuptake_{cyano}$	0.08	$Uptakemax_{bact}$	0.06	Tempref	0.08
$KTgr_{cyano}$	-0.15	$KTgr_{non\text{-}cy}$	-0.14	maxgrazing	-0.15	$Tref_{cyano}$	-0.25	β_N	-0.18	β_N	-0.17
$Pmax_{non\text{-}cy}$	-0.19	$KTgr_{cyano}$	-0.18	$KTgr_{cyano}$	-0.19	$Vsettling_{cyano}$	-0.34	$KTgr_{cyano}$	-0.21	$KTgr_{cyano}$	-0.29
$Vsettling_{cyano}$	-0.21	$Pmax_{non\text{-}cy}$	-0.22	$Pmax_{non\text{-}cy}$	-0.25	$Vsettling_{non\text{-}cy}$	-0.53	$Vsettling_{cyano}$	-0.33	$Pmax_{non\text{-}cy}$	-0.30
$Vsettling_{non\text{-}cy}$	-0.25	$Vsettling_{cyano}$	-0.27	$Vsettling_{cyano}$	-0.29	βp	-0.54	$Pmax_{non\text{-}cy}$	-0.35	$Vsettling_{cyano}$	-0.32
βp	-0.36	$Vsettling_{non\text{-}cy}$	-0.32	$Vsettling_{non\text{-}cy}$	-0.34	$Pmax_{non\text{-}cy}$	-0.56	$Vsettling_{non\text{-}cy}$	-0.41	$Vsettling_{non\text{-}cy}$	-0.40
β_N	-0.47	βp	-0.39	βp	-0.41	β_N	-1.03	βp	-0.46	βp	-0.44
$Tref_{cyano}$	-0.48	$Tref_{cyano}$	-0.49	$Tref_{cyano}$	-0.59	$Nmin_{cyano}$	-1.05	$Tref_{cyano}$	-0.74	$Tref_{cyano}$	-0.75
Cyanobacteria chl *a*											
$grthmax_{cyano}$	1.17	$grthmax_{cy}$	1.16	$grthmax_{cyano}$	1.18	$Nmax_{cyano}$	1.11	$grthmax_{cyano}$	1.07	$grthmax_{cyano}$	1.11
$\alpha_{ON\ BACT}$	0.84	$\alpha_{ON\ BACT}$	0.92	$\alpha_{ON\ BACT}$	0.74	$grthmax_{cyano}$	1.11	$Pmax_{non\text{-}cy}$	0.54	$Vsettling_{non\text{-}cy}$	0.51
$Tref_{non\text{-}cy}$	0.49	$Tref_{non\text{-}cy}$	0.47	$Vsettling_{non\text{-}cy}$	0.55	$Pmax_{non\text{-}cy}$	0.68	$Vsettling_{non\text{-}cy}$	0.52	$Pmax_{non\text{-}cy}$	0.47
$Vsettling_{non\text{-}cy}$	0.39	$Vsettling_{non\text{-}cy}$	0.46	$Pmax_{non\text{-}cy}$	0.51	$Vsettling_{non\text{-}cy}$	0.56	βp	0.28	$\alpha_{ON\ BACT}$	0.32
$Pmax_{non\text{-}cy}$	0.36	$Pmax_{non\text{-}cy}$	0.45	$Tref_{non\text{-}cy}$	0.41	βp	0.39	$\alpha_{ON\ BACT}$	0.27	βp	0.23
$KN_{non\text{-}cy}$	0.24	$Ik_{non\text{-}cy}$	0.22	$Ik_{non\text{-}cy}$	0.28	$Pmaxuptake_{cyano}$	0.31	$KP_{non\text{-}cy}$	0.24	$Pmaxuptake_{cyano}$	0.22
mp_{cyano}	-0.30	β_N	-0.47	β_N	-0.49	$grthmax_{non\text{-}cy}$	-0.82	β_N	-0.63	$Nmax_{cyano}$	-0.59
$grthmax_{non\text{-}cy}$	-0.46	$Nmax_{cyano}$	-0.50	$Nmax_{cyano}$	-0.51	$Vsettling_{cyano}$	-1.28	$Nmax_{cyano}$	-0.63	β_N	-0.60
$KTgr_{cyano}$	-0.61	$grthmax_{non\text{-}cy}$	-0.54	$grthmax_{non\text{-}cy}$	-0.54	$KTgr_{cyano}$	-1.74	$grthmax_{non\text{-}cy}$	-0.66	$grthmax_{non\text{-}cy}$	-0.72
$Vsettling_{cyano}$	-0.69	$KTgr_{cyano}$	-0.83	$KTgr_{cyano}$	-0.95	$Tref_{cyano}$	-3.01	$KTgr_{cyano}$	-1.29	$KTgr_{cyano}$	-1.18
$Tref_{cyano}$	-1.51	$Vsettling_{cyano}$	-1.00	$Vsettling_{cyano}$	-1.07	$Nmin_{cyano}$	-3.06	$Vsettling_{cyano}$	-1.29	$Vsettling_{cyano}$	-1.25
β_N	-1.65	$Tref_{cyano}$	-2.02	$Tref_{cyano}$	-2.62	β_N	-3.44	$Tref_{cyano}$	-4.76	$Tref_{cyano}$	-4.24

ultimately provide a useful tool for designing management policies and restoration practices. However, the considerable uncertainty pertaining to any complex overparameterized modeling construct can be a major impediment for eliciting the straightforward scientific answers required to guide management decisions, and thus the critical evaluation of the inference drawn along with the impartial differentiation between real knowledge gained and existing knowledge gaps are critical steps in this endeavour (Arhonditsis et al., 2007). In this regard, we believe that the key findings of our process-based model should be critically evaluated against the existing empirical information from the studied lagoon in order to put the derived ecosystem characterization into perspective as well as to guide future model refinements.

One of the founding assumptions of our work is that the ecological processes in the studied shallow oligohaline lagoon resemble to those in lake ecosystems, and thus the local restoration efforts can benefit from the eutrophication management paradigm in limnology. In this context, a study comprising 35 long-term lake re-oligotrophication cases (mostly from north-temperate lakes) showed that a new equilibrium for total phosphorus and nitrogen may be reached after 10 – 15 and < 5 years, respectively (Jeppesen et al., 2005). The same study was able to tease out broader food web patterns, such as a decrease in phytoplankton biomass, an increase in the zooplankton to phytoplankton biomass ratio, probably caused by higher zooplankton grazing rates, which could in turn be attributed to an overall fish biomass decline as well as a substantial increase in the abundance of piscivorous fish (Jeppesen et al., 2005). The reduction in P loadings in the warm-temperate Albufera de Valencia has resulted in a decline of TP concentrations similar to that reported by Jeppesen et al. (2005). However, the food web has demonstrated fundamentally different response; for example, the zooplankton to phytoplankton biomass ratio remained lower than in northern temperate shallow lakes and the predominance of omnivorous fish species (*Mugil cephalus* L., *Liza aurata* Risso and *Cyprinus carpio* L.) was distinctly different from the abundance increase in piscivorous species typically observed in north temperate lakes after nutrient loading reduction (Blanco et al., 2003; Romo et al., 2005). Consistent with these observations, warm lakes have been found to be generally dominated by omnivorous fish species (regardless of their trophic state) and to host fewer piscivores. Of equal importance is the fact that the partial overlap of species niches within and among trophic levels, the higher fish density, and the greater number of fish cohorts per year in warm lakes typically result in higher predation pressure on zooplankton relative to the northern temperate lakes (Jeppesen et al., 2007a). Consequently, the likelihood of strong trophic cascades that could mediate the control of algae by larger herbivorous zooplankton may be reduced in warm lakes. In particular, the higher fish predation rates in Albufera resulted in a zooplankton community that was primarily dominated by small species of rotifers and cyclopoid copepods, with limited capacity to confine the levels of primary production. Along the same line of reasoning, experimental data on a shallow Mediterranean lake indicated that the nutrient levels required for the loss of macrophytes are lower than those needed in north temperate lakes, i.e., TP < 0.1–0.05 mg TP L^{-1} (Romo et al., 2004). These findings suggest that drawing parallels between north and warm temperate lakes may not be a straightforward task and the response of the latter group of water bodies (south temperate, subtropical, and tropical lakes) to management actions entails considerable uncertainties (Jeppesen et al., 2003).

As previously mentioned, omnivorous species, such as *Mugil cephalus* L., *Liza aurata* Risso, and *Cyprinus carpio* L. dominate the fish community in Albufera de Valencia, whereas potentially piscivorous species, such as *Sander lucioperca* L. and *Dicentrarchus labrax* (L.), are scarce (Blanco et al., 2003). During the summer period, the diet composition of both *Liza aurata* Risso and *Cyprinus carpio* L. was mainly based on detritus (≈50%) and to a lesser extent in sediment (≈10%) and zooplankton (5–15%). However, detritus contributed only 25% to the diet of *Mugil cephalus,* while zooplankton made up for 30% of its diet, with copepods amounting to more than 80% of the latter food items (Blanco et al., 2003). This situation changed in spring, when *L. aurata* and especially *Cyprinus carpio* fed predominantly on large zooplankton (mainly *Daphnia magna*) as the abundance of this group increased (Blanco et al., 2003). In this regard, it is not surprising that the zooplankton to phytoplankton biomass ratio is smaller in the studied lagoon than in other northern temperate systems (Romo et al., 2005). Aside from the

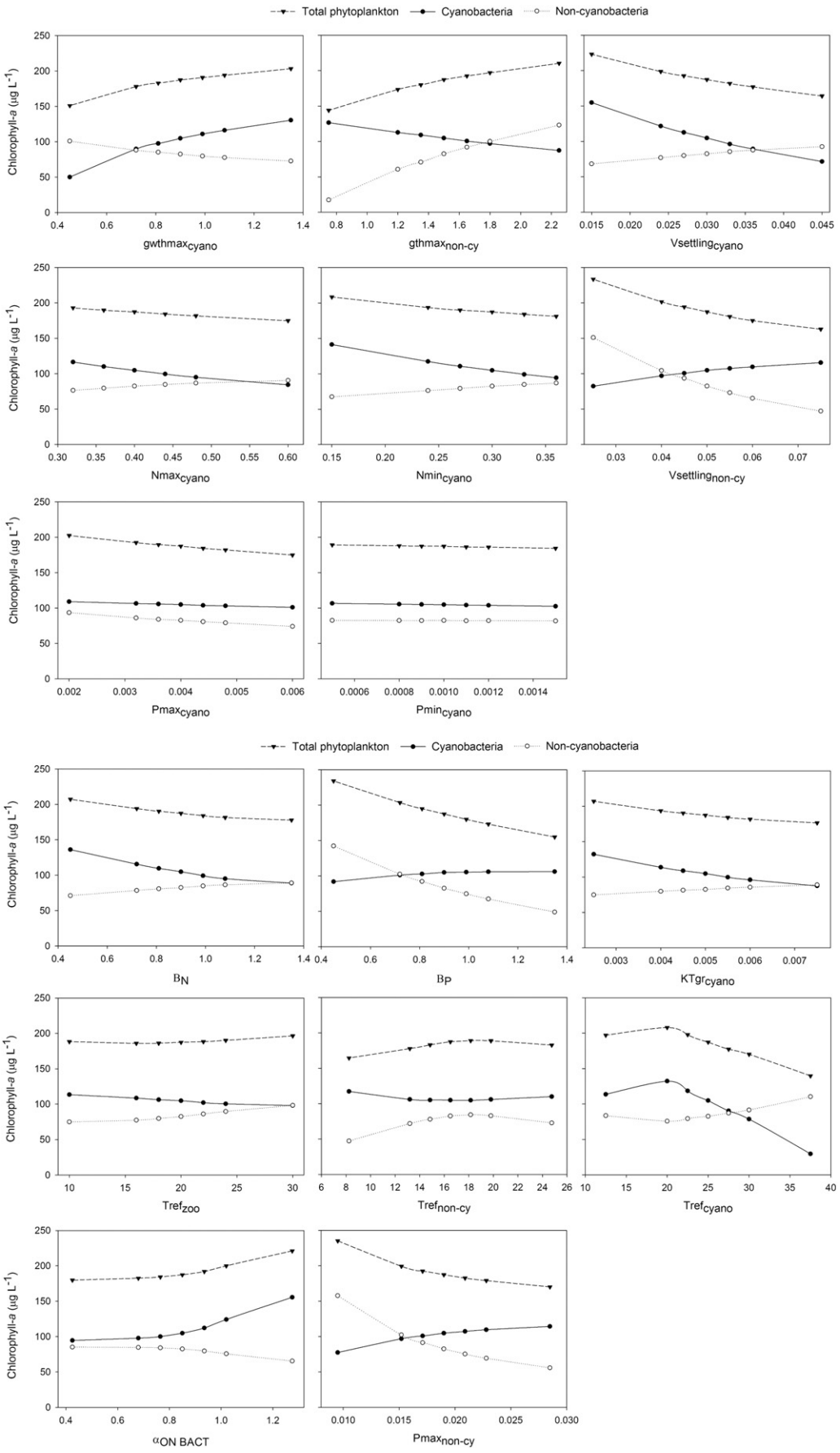

Fig. 6. Changes of the mean annual total chlorophyll *a*, cyanobacteria, and non-cyanobacteria concentrations induced by ±10, 20 and 50% variations of selected parameters relative to the values assigned after the model calibration.

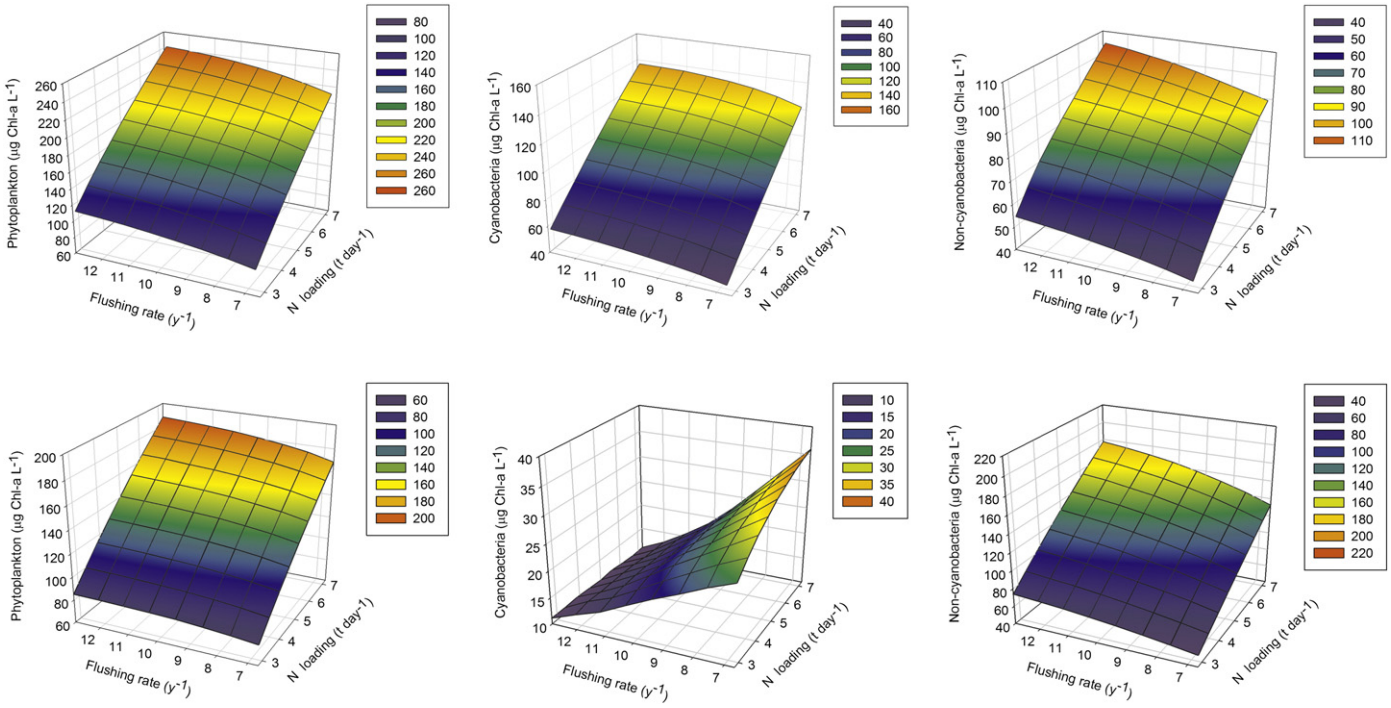

Fig. 7. Comparison between model predictions for mean annual (upper panels) and mean February-March (lower panels) total chlorophyll *a* (left panels), cyanobacteria (central panels) and non-cyanobacteria (right panels) concentrations under a wide range of loading and flushing conditions. [The nutrient loading variations correspond to flow-weighted mean concentrations from 4.4 to 11.3 mg TN L^{-1} and 130 to 340 µg TP L^{-1}, respectively.]

high fish predation pressure exerted on zooplankton in warm eutrophic lakes, resulting in herbivorous communities dominated by small species, top-down control is often impeded by non-edible algae (filamentous cyanobacteria). In Albufera de Valencia, filamentous cyanobacteria dominate the system during most of the annual cycle, and thus inhibit *Daphnia magna* feeding by mechanical interference (Sahuquillo et al., 2007). However, after increased flushing favoured the growth of edible algae in late winter (see also lower panels in our Fig. 7), *Daphnia magna* was found to contribute to the occurrence of clear-water phases in the lagoon (Miracle and Sahuquillo, 2002). This finding indicates that top-down control might still be achieved under a combination of favourable conditions, thereby mediating the establishment of a clear water phase in the lagoon.

Among the array of restoration strategies that could be implemented, nutrient control has been highlighted as a priority in eutrophic warm shallow systems comparing with similar lakes at higher latitudes (Moss et al., 2004; Romo et al., 2005). Nonetheless, nutrient loading reduction has often proven inadequate to achieve full restoration and additional management actions might be needed (Gulati and van Donk, 2002). Given that the hydrological cycle is strongly regulated by the requirements of rice cultivation, the modulation of the flushing rates may offer an effective management tool in Albufera de Valencia. The maintenance of hydraulic conditions similar to those leading to the late winter/early spring clear-water event in our dataset has been proposed as a possible measure to achieve light conditions that would allow the establishment of macrophytes; namely, turbidity-tolerant charophyte species which in turn would potentially facilitate the submerged vegetation recovery (Miracle et al., 2012; Rodrigo and Alonso-Guillén, 2013). Our analysis suggests that the current annual net loading into the system is positive, and therefore faster flushing rates do not necessarily result in a net decrease of the ambient nutrient levels on an annual basis. Thus, the fueling of algal growth by the inflowing nutrients is not fully counterbalanced by the amount of particulate material flushed out of the lagoon. Nonetheless, if we use monthly resolution to examine the prevailing conditions, we note that there is considerable intra-annual variability in regard to the net loading (Fig. 8), and thus the likelihood of the dilution effects associated with faster flushing rates to be partly responsible for the occurrence of clear water events cannot be ruled out.

The terrestrial loading was the main contributor of phosphate input into the water column (>90%), while the reflux from the sediments was smaller than that originated from other recycling mechanisms (mineralization and plankton basal metabolism). While this finding is conceptually on par with modeling projections for the shallow Lake Okeechobee (James et al., 1997), we note that (unlike the latter system) the phosphate originated from recycling mechanisms was not enough to meet the phytoplankton demands, and thus the external loading represents a reliable phosphorus source for autotrophic growth in Albufera de Valencia. Similar inference could be drawn with respect to the terrestrial nitrogen loadings and their causal linkage with the phytoplankton biomass. Nonetheless, our analysis also pinpointed the role of bacteria-mediated mineralization as a critical supplier of bioavailable nitrogen in the lagoon; a finding that is supported by empirical evidence of a significant correlation between bacterial biomass and ambient NO_3, NO_2 and NH_4 levels at the daily scale in Albufera de Valencia (Onandia et al., 2014a). Importantly, although phosphorus has long been considered the limiting nutrient in lakes, the distinct summer drop of the dissolved nitrogen levels suggests that the lagoon may periodically experience nutrient co-limitation or nitrogen limitation. Consistent with this hypothesis, recent work in the lagoon has reported sharp dissolved nitrogen decline concomitant to the appearance of heterocystous cyanobacteria, such as *Cylindrospermopsis raciborskii*, and a contemporary diminution in primary productivity (Onandia et al., 2014b). Thus, our analysis not only renders support to the notion that the external nutrient control should be a priority in the warm temperate Albufera de Valencia, but also underscores the importance of the restoration efforts to focus on both nitrogen and phosphorus loadings.

The latter recommendation is reinforced by the fact that the recovery of submerged macrophytes after loading reduction is more likely to occur at moderately high total phosphorus when total nitrogen

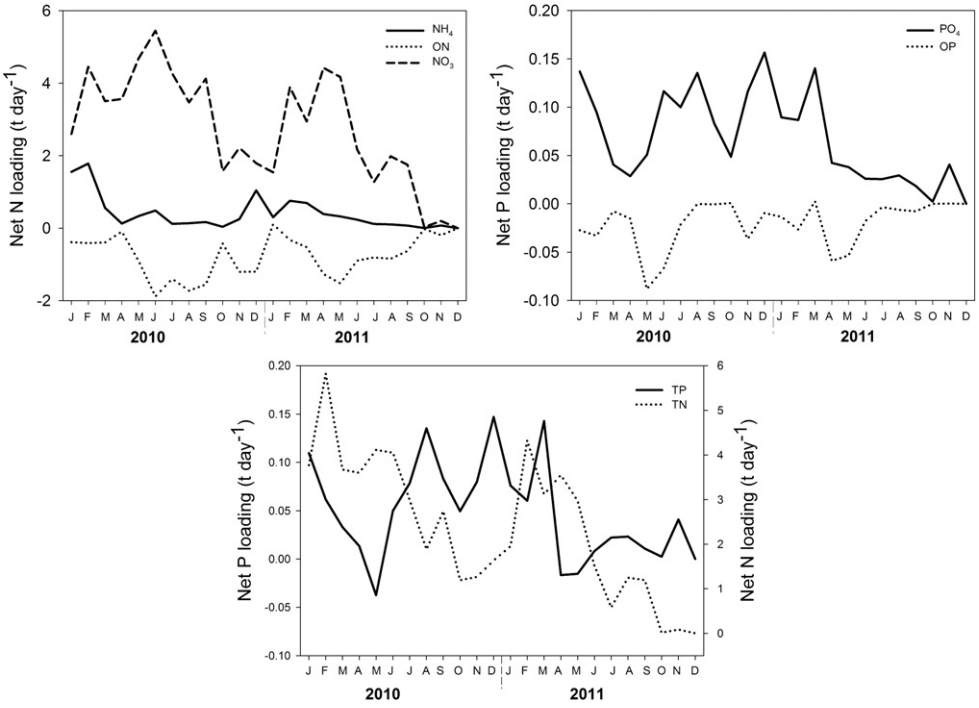

Fig. 8. Net nitrogen (upper left), phosphorus (upper right), and total nitrogen and phosphorus (lower panel) loadings into Albufera de Valencia.

loading is low (Jeppesen et al., 2007a and references therein). In a study of Danish shallow lakes, macrophyte cover was fairly low when mean summer TN exceeded the level of 2 mg N L^{-1} and TP was greater than 0.2 mg P L^{-1}, while an important macrophyte coverage was observed when TN concentrations were below 1-2 mg N L^{-1}, irrespective of the TP concentrations, which however ranged from 0.03 to 0.2 mg P L^{-1} (González Sagrario et al., 2005). The explanation for the macrophyte elimination at TN > 1-2 mg N L^{-1} and TP ≥ 0.2 mg P L^{-1} might be the alleviation of nutrient limitation, leading to excessive phytoplankton and periphyton growth and subsequently to severe light attenuation (González Sagrario et al., 2005). Further, lakes characterized by inorganic nitrogen to TP ratios lower than 7, showed that inorganic N usually remains below 0.1 mg L^{-1} when TP is between 0.015 mg L^{-1} and 0.12 mg L^{-1}, suggesting that N limitation of algae is likely within this TP range (Jeppesen et al., 2007b). Based on these results, Jeppesen et al. (2007b) highlighted the critical role of N in obtaining a clear-water state, especially in systems with an agricultural watershed, where it might be challenging to achieve sufficiently low P levels to eliminate the impact of N. In Albufera de Valencia, our estimates of the current terrestrial areal nitrogen and phosphorus loads are 90 g N m^{-2} y^{-1} and 2.7 g P m^{-2} y^{-1}, respectively, while the observed TN surpassed the level of 2 mg N L^{-1} during the summer of both 2010 and 2011. Clearly, more work needs to be done in order to bring the nutrient loading regime close to levels that will trigger visible water quality improvements in the lagoon.

The introduction of macrophytes represents another widespread restoration strategy (Hilt et al., 2006; Ozimek et al., 1990). Macrophytes stabilize water transparency by different mechanisms, e.g., reduction of sediment resuspension, increase in sedimentation, nutrient competition with algae, and shelter provision for zooplankton against fish predation (Ibelings et al., 2007). In Albufera de Valencia, poor light conditions primarily prevent the growth of macrophytes during most of the annual cycle, although sediment characteristics and wind stress might also modulate the extent of their proliferation (Hilt et al., 2006; Schutten et al., 2004). The recolonization of submerged macrophytes should probably target shallow areas close to the shoreline, where light availability is higher and emerged macrophytes, such as *Phragmites australis, Typha angustifolia, Typhta latifolia or Scirpus lacustris*, lessen the mechanical wind stress. Further, another critical factor for the recovery of submerged vegetation is the potential of sediments to host charophytes, an aspect that has been recently assessed in Albufera de Valencia. The upper sediment layers, deposited throughout the eutrophication era of the lagoon, have the capacity to sustain the vegetative growth of *Chara hispida* and *Chara vulgaris* and promote the germination of *Chara aspera* and *Chara baltica* (Rodrigo and Alonso-Guillén, 2013). Currently, our model does not explicitly consider the role of macrophytes, but future model augmentation should account for their potential contribution to the successful establishment of a clear water state.

The role of the sediments is also of great importance in eutrophic shallow systems with high sediment surface to water column ratio. After nutrient reduction, lake recovery is often delayed because of the internal loading induced by diverse mechanisms (Søndergaard et al., 2003, 2005). The Albufera model predicted a linear response to the potential external loading reductions, but the chlorophyll *a* remained in fairly high levels (90 μg L^{-1}), even after a significant external loading reduction (up to 50 %). These results indicate that the system displays a moderate hysteresis in relation to the exogenous N and P input changes, which suggests that internal loading would (at least partly) hinder the response under the scenarios examined. The magnitude of the internal loading is determined by the morphometry of the system, the flushing rates, the sediment characteristics, the nutrient enrichment and trophic state (Marsden, 1989). For example, the combination of a short residence time with a high pH buffering capacity in the shallow Lake Veluwe in the Netherlands reduced the impact of internal P loading (Ibelings et al., 2007), and could similarly affect the Albufera de Valencia; a system that shares similar characteristics, such as the elevated flushing rate (≈8.9 y^{-1}) and high alkalinity (≈25 mg L^{-1}). Among the complex array of factors that shape the sediment diagenesis processes, it is important to shed light on the spatial and temporal nutrient distribution as well as their chemical fractioning. Certain forms such as loosely sorbed organic and inorganic fractions or iron-bound and redox-sensitive P are regarded as potentially mobile (Søndergaard et al., 2001). Albufera de Valencia is a well-mixed lagoon with practically negligible spatial variations of its physicochemical parameters (Onandia et al., 2014). The occurrence of anoxia is restricted to a very limited period of a few night hours during the mid-summer, and therefore the

internal release under anaerobic conditions likely represents a minor contributor to the nutrient budget in the water column. Nonetheless, the available information comprises measurements with limited temporal or spatial resolution and the sediment-water column interactions warrant further investigation in Albufera de Valencia (del Barrio Fernández et al., 2012; Monerris, 1998).

We conclude by emphasizing that the representation of the role of zooplankton in the stands out as one of the critical future augmentations of our eutrophication model. In particular, the succession patterns between the two different zooplankton community structures associated with the clear water events and the rest of the annual cycle is one of the critical features to characterize the phytoplankton-zooplankton interactions in the system. The second major feature is the explicit consideration of macrophytes and the reproduction of their interplay with the physical, chemical, and biological components of the system, as the nutrient loading reduction plans take effect. Model-based approaches to eutrophication management are intended either for heuristic purposes, illuminating trophic interrelationships and pinpointing unexpected ramifications of management actions, or for predictive uses, aiming to offer a formal examination of policy relevant ecosystem responses (Arhonditsis and Brett, 2004). While the Albufera model could ultimately be used for the latter type of questions, the substantial uncertainty associated with several critical inputs (loading estimates, optimal model structure) poses constraints on its use and also invites a rigorous assessment of some of the assumptions made during its development. Acknowledging the knowledge gaps from the system as well as the uncertainties associated with any modeling endeavour, the present exercise should rather be viewed as the beginning of our efforts towards the development of a credible management tool for the shallow lagoon of Albufera de Valencia.

Acknowledgements

We thank E. Vicente for his valuable assistance during the whole data collection process (field and laboratory). We also thank J.M. Soria, X. Soria and the rangers of the Oficina Tecnica Devesa-Albufera for their help in the field. We are likewise thankful to J.M .Soria and Olga Kramer for chemical analyses assistance and data and to C. Blanco, M.D. Sendra and Alfonso M. for bacteria, phytoplankton and zooplankton data. We thank Weitao Zhang and Dong-Kyun Kim for their assistance and valuable comments during the model development process. We also thank the Agencia Estatal de Metereología (AEMET) for providing data on day length, precipitation, evaporation and wind and the Confederación Hidrográfica del Júcar for hydrological data. This work was supported by the Spanish Ministry of Economy and Competitiveness through the project CGL2009-12229 and grant BES-2010- 481 032212.

References

APHA (American Public Health Association), 1992. Standard methods for the examination of water and wastewater. 18th edition. American Public Health Association, Washington D.C.
Arhonditsis, G.B., Brett, M.T., 2004. Evaluation of the current state of mechanistic aquatic biogeochemical modeling. Mar. Ecol. Prog. Ser. 271, 13–26.
Arhonditsis, G.B., Brett, M.T., 2005a. Eutrophication model for Lake Washington (USA) Part I. Model description and sensitivity analysis. Ecol. Model. 187, 140–178.
Arhonditsis, G.B., Brett, M.T., 2005b. Eutrophication model for Lake Washington (USA) Part II - model calibration and system dynamics analysis. Ecol. Model. 187, 179–200.
Arhonditsis, G., Tsirtsis, G., Karydis, M., 2002. The effects of episodic rainfall events to the dynamics of coastal marine ecosystems: applications to a semi-enclosed gulf in the Mediterranean Sea. J. Mar. Syst. 35, 183–205.
Arhonditsis, G.B., Qian, S.S., Stow, C.A., Lamon, E.C., Reckhow, K.H., 2007. Eutrophication risk assessment using Bayesian calibration of process-based models: application to a mesotrophic lake. Ecol. Model. 208, 215–229.
Arhonditsis, G.B., Papantou, D., Zhang, W., Perhar, G., Massos, E., Shi, M., 2008. Bayesian calibration of mechanistic aquatic biogeochemical models and benefits for environmental management. J. Mar. Syst. 73, 8–30.
Beklioglu, M., Ince, O., Tuzun, I., 2003. Restoration of the eutrophic Lake Eymir, Turkey, by biomanipulation after a major external nutrient control I. Hydrobiologia 490, 93–105.
Berounsky, V.M., Nixon, S.W., 1990. Temperature and the annual cycle of nitrification in waters of Narragansett Bay. Limnol. Oceanogr. 35, 1610–1617.
Blanco, S., Romo, S., 2006. Ictiofauna del lago de la Albufera de Valencia: evolución histórica y situación actual. Bol. R. Soc. Esp. Hist. Nat. (Sección Biol.) 101, 45–56.
Blanco, S., Romo, S., Villena, M.-J., Martínez, S., 2003. Fish communities and food web interactions in some shallow Mediterranean lakes. Hydrobiologia 506, 473–480.
Bottrell, H.c., 1976. A review of some problems in zooplankton production studies. Nor. J. Zool. 24, 419–456.
Breukelaar, A.W., Lammens, E.H., Breteler, J.G.K., Tatrai, I., 1994. Effects of benthivorous bream (*Abramis brama*) and carp (*Cyprinus carpio*) on sediment resuspension and concentrations of nutrients and chlorophyll a. Freshw. Biol. 32, 113–121.
Carpenter, S.R., Caraco, N.F., Correll, D.L., Howarth, R.W., Sharpley, A.N., Smith, V.H., 1998. Nonpoint pollution of surface waters with phosphorus and nitrogen. Ecol. Appl. 8, 559–568.
Cerco, C.F., Cole, T.M., 1994. CE-QUAL-ICM: A 3-dimensional eutrophication model, version 1.0. User's Guide. US Army Corps of Engineers Waterways Experiments Station, Vicksburgh, MS.
Chao, X., Jia, Y., Shields Jr., F.D., Wang, S.S., Cooper, C.M., 2008. Three-dimensional numerical modeling of cohesive sediment transport and wind wave impact in a shallow oxbow lake. Adv. Water Resour. 31, 1004–1014.
Chen, C., Ji, R., Schwab, D.J., Beletsky, D., Fahnenstiel, G.L., Jiang, M., Johengen, T.H., Vanderploeg, H., Eadie, B., Budd, J.W., 2002. A model study of the coupled biological and physical dynamics in Lake Michigan. Ecol. Model. 152, 145–168.
del Barrio Fernández, P., Gómez, A.G., Alba, J.G., Díaz, C.Á., Revilla Cortezón, J.A., 2012. A model for describing the eutrophication in a heavily regulated coastal lagoon. Application to the Albufera of Valencia (Spain). J. Environ. Manag. 112, 340–352.
Dickman, M., 1969. Some effects of lake renewal on phytoplankton productivity and species composition. Limnol. Oceanogr. 14, 660–666.
Dillon, P., 1975. The phosphorus budget of Cameron Lake, Ontario: The importance of flushing rate to the degree of eutrophy of lakes. Limnol. Oceanogr. 20, 28–39.
Dodds, W.K., Bouska, W.W., Eitzmann, J.L., Pilger, T.J., Pitts, K.L., Riley, A.J., Schloesser, J.T., Thornbrugh, D.J., 2008. Eutrophication of US freshwaters: analysis of potential economic damages. Environ. Sci. Technol. 43, 12–19.
Downing, J.A., Rigler, F.H., 1984. A Manual on Methods for the Assessment of Second Productivity in Fresh Waters. second edition. Blackwell Scientific Publications, Oxford.
Dröscher, I., Finlay, K., Patoine, A., Leavitt, P., 2008. *Daphnia* control of the spring clear-water phase in six polymictic lakes of varying productivity and size. Int. Ver. Theor. 30, 186–190.
Dröscher, I., Patoine, A., Finlay, K., Leavitt, P.R., 2009. Climate control of the spring clear-water phase through the transfer of energy and mass to lakes. Limnol. Oceanogr. 54, 2469–2480.
Dumont, H.J., Van de Velde, I., Dumont, S., 1975. The dry weight estimate of biomass in a selection of Cladocera, Copepoda and Rotifera from the plankton, periphyton and benthos of continental waters. Oecologia 19, 75–97.
Escribá, D., 1988. Hidráulica para Ingenieros. first edition. Editorial Bellisco, Madrid.
Fasham, M., Ducklow, H., McKelvie, S., 1990. A nitrogen-based model of plankton dynamics in the oceanic mixed layer. J. Mar. Res. 48, 591–639.
García, M., Vicente, E., Miracle, M.R., 1984. Sucesión estacional del fitoplancton de la Albufera de Valencia. An. Biol. 2 (s.e.2), 91–100.
González Sagrario, M.A., Jeppesen, E., Gomà, J., Søndergaard, M., Jensen, J.P., Lauridsen, T., Landkildehus, F., 2005. Does high nitrogen loading prevent clear-water conditions in shallow lakes at moderately high phosphorus concentrations? Freshw. Biol. 50, 27–41.
Gudimov, A., Stremilov, S., Ramin, M., Arhonditsis, G.B., 2010. Eutrophication risk assessment in Hamilton Harbour: system analysis and evaluation of nutrient loading scenarios. J. Great Lakes Res. 36, 520–539.
Gulati, R.D., Van Donk, E., 2002. Lakes in the Netherlands, their origin, eutrophication and restoration: state-of-the-art review. Hydrobiologia 478, 73–106.
Hamilton, D.P., Schladow, S.G., 1997. Prediction of water quality in lakes and reservoirs. Part I—Model description. Ecol. Model. 96, 91–110.
Hessen, D., Lyche, A., 1991. Inter-and intraspecific variations in zooplankton element composition. Arch. Hydrobiol. 121, 343–353.
Hillebrand, H., Durselen, C.D., Kirschtel, D., Pollingher, U., Zohary, T., 1999. Biovolume calculation for pelagic and benthic microalgae. J. Phycol. 35, 403–424.
Hilt, S., Gross, E.M., Hupfer, M., Morscheid, H., Mählmann, J., Melzer, A., Poltz, J., Sandrock, S., Scharf, E.-M., Schneider, S., 2006. Restoration of submerged vegetation in shallow eutrophic lakes–A guideline and state of the art in Germany. Limnologica 36, 155–171.
Ibelings, B.W., Portielje, R., Lammens, E.H., Noordhuis, R., van den Berg, M.S., Joosse, W., Meijer, M.L., 2007. Resilience of alternative stable states during the recovery of shallow lakes from eutrophication: Lake Veluwe as a case study. Ecosystems 10, 4–16.
Ijima, T., Tang, F.L., 1966. Numerical calculation of wind waves in shallow water. Coast. Eng. Proc. 1, 10.
ISO (International Organization for Standardization), 1997. Water analysis - Guidelines for the determination of total organic carbon (TOC) and dissolved organic carbon (DOC). ISO EN 1484.ISO, Geneva.
Jagtman, E., Van der Molen, D., Vermij, S., 1992. The influence of flushing on nutrient dynamics, composition and densities of algae and transparency in Veluwemeer, The Netherlands. In: van Liere, L., Gulati, R. (Eds.), Restoration and Recovery of Shallow Eutrophic Lake Ecosystems in The Netherlands. Springer, pp. 187–196.
James, R.T., Martin, J., Wool, T., Wang, P., 1997. A sediment resuspension and water quality model of Lake Okeechobee. J. Am. Water Resour. Assoc. 33, 661–678.
Jassby, A.D., Platt, T., 1976. Mathematical formulation of the relationship between photosynthesis and light for phytoplankton. Limnol. Oceanogr. 21, 540–547.
Jeppesen, E., Søndergaard, M., Jensen, J.P., Lauridsen, T.L., 2003. Recovery from eutrophication. In: Kumagai, M., Vincent, W.F. (Eds.), Freshwater Management. Global versus Local Perspectives. Springer-Verlag, New York, pp. 1–16.

Jeppesen, E., Søndergaard, M., Jensen, J.P., Havens, K.E., Anneville, O., Carvalho, L., Coveney, M.F., Deneke, R., Dokulil, M.T., Foy, B., 2005. Lake responses to reduced nutrient loading – an analysis of contemporary long-term data from 35 case studies. Freshw. Biol. 50, 1747–1771.

Jeppesen, E., Meerhoff, M., Jacobsen, B., Hansen, R., Søndergaard, M., Jensen, J., Lauridsen, T., Mazzeo, N., Branco, C., 2007a. Restoration of shallow lakes by nutrient control and biomanipulation – the successful strategy varies with lake size and climate. Hydrobiologia 581, 269–285.

Jeppesen, E., Søndergaard, M., Meerhoff, M., Lauridsen, T.L., Jensen, J.P., 2007b. Shallow lake restoration by nutrient loading reduction – some recent findings and challenges ahead. Hydrobiologia 584, 239–252.

Jorgensen, S.E., Nilsen, S.N., Jorgensen, L.A., 1991. Handbook of ecological parameters and ecotoxicology. sixth edition. Elsevier, Amsterdam.

Kim, D.-K., Zhang, W., Rao, Y.R., Watson, S., Mugalingam, S., Labencki, T., Dittrich, M., Morley, A., Arhonditsis, G.B., 2013. Improving the representation of internal nutrient recycling with phosphorus mass balance models: A case study in the Bay of Quinte, Ontario, Canada. Ecol. Model. 256, 53–68.

Lampert, W., Fleckner, W., Rai, H., Taylor, B.E., 1986. Phytoplankton control by grazing zooplankton: a study on the spring clear-water phase. Limnol. Oceanogr. 31, 478–490.

Lampert, W., Sommer, U., Haney, J.F., 1997. Limnoecology: the ecology of lakes and streams. second edition. Oxford University Press, New York.

Latja, R., Salonen, K., 1978. Carbon analysis for the determination of individual biomasses of planktonic animals. Proceedings: Congress in Denmark 1977. Int. Ver. Theor. Angew. Limnol. 20.

Marsden, M.W., 1989. Lake restoration by reducing external phosphorus loading: the influence of sediment phosphorus release. Freshw. Biol. 21, 139–162.

Martín, M., Oliver, N., Hernández-Crespo, C., Gargallo, S., Regidor, M., 2013. The use of free water surface constructed wetland to treat the eutrophicated waters of lake L'Albufera de Valencia (Spain). Ecol. Eng. 50, 52–61.

McNeary, W.W., Erickson, L.E., 2013. Sustainable management of algae in eutrophic ecosystems. J. Environ. Prot. 4, 9–19.

Mehta, A.J., Partheniades, E., 1982. Resuspension of deposited cohesive sediment beds. Coast. Eng. Proc. 1, 18.

Mian, M.H., Yanful, E.K., 2004. Analysis of wind-driven resuspension of metal mine sludge in a tailings pond. J. Environ. Eng. Sci. 3, 119–135.

Miracle, M.R., Sahuquillo, M., 2002. Changes of life-history traits and size in *Daphnia magna* during a clear-water phase in a hypertrophic lagoon (Albufera of Valencia, Spain). Verh. Int. Ver. Limnol. 28, 1203–1208.

Miracle, M.R., Sahuquillo, M., Alfonso, T., Sendra, M.D., 2012. Las fases claras a l'Albufera: una via per la seua recuperació. In: Català, J. (Ed.), La Universitat de València i els seus entorns naturals: els parcs naturals de l'Albufera, el Túria i la Serra Calderona. Universitat de València, València, pp. 96–99.

Monerris, M.M., 1998. Modelación de la calidad en aguas superficiales. Aplicación al caso de La Albufera de Valencia. Departamento de Ingeniería Química. Universitat de València, València.

Morales-Baquero, R., Pulido-Villena, E., Reche, I., 2006. Atmospheric inputs of phosphorus and nitrogen to the southwest Mediterranean region: Biogeochemical responses of high mountain lakes. Limnol. Oceanogr. 51, 830–837.

Moss, B., Stephen, D., Alvarez, C., Becares, E., Bund, W.V.D., Collings, S., Donk, E.V., Eyto, E.D., Feldmann, T., Fernández-Aláez, C., 2003. The determination of ecological status in shallow lakes – a tested system (ECOFRAME) for implementation of the European Water Framework Directive. Aquat. Conserv. 13, 507–549.

Moss, B., Stephen, D., Balayla, D., Bécares, E., Collings, S., Fernández-Aláez, C., Fernández-Aláez, M., Ferriol, C., García, P., Gomá, J., 2004. Continental-scale patterns of nutrient and fish effects on shallow lakes: synthesis of a pan-European mesocosm experiment. Freshw. Biol. 49, 1633–1649.

Moustaka-Gouni, M., Vardaka, E., Michaloudi, E., Kormas, K.A., Tryfon, E., Mihalatou, H., Gkelis, S., Lanaras, T., 2006. Plankton food web structure in a eutrophic polymictic lake with a history in toxic cyanobacterial blooms. Limnol. Oceanogr. 51, 715–727.

Omlin, M., Brun, R., Reichert, P., 2001. Biogeochemical model of Lake Zürich: sensitivity, identifiability and uncertainty analysis. Ecol. Model. 141, 105–123.

Onandia, G., Miracle, M.R., Blasco, C., Vicente, E., 2014a. Diel and seasonal variations in bacterial production in a hypertrophic shallow lagoon. Aquat. Microb. Ecol. 72, 255–267.

Onandia, G., Miracle, M.R., Vicente, E., 2014b. Primary production under hypertrophic conditions and its relationship with bacterial production. Aquatic Ecology 48, 447–463.

Orcutt, J.D., Porter, K.G., 1983. Diel vertical migration by zooplankton: constant and fluctuating temperature effects on life history parameters of *Daphnia*. Limnol. Oceanogr. 28, 720–730.

Ozimek, T., Gulati, R.D., van Donk, E., 1990. Can macrophytes be useful in biomanipulation of lakes? The Lake Zwemlust example. Biomanipulation tool for water management. Dev. Hydrobiol. 61, 339–407.

Padisák, J., Köhler, J., Hoeg, S., 1999. Effect of changing flushing rates on development of late summer *Aphanizomenon* and *Microcystis* populations in a shallow lake, Müggelsee, Berlin, Germany. In: Tundisi, J.G., Straskraba, M. (Eds.), Theoretical reservoir ecology and its applications. Backhuys Publishers, São Carlos, pp. 411–423.

Pardo, L., 1942. La Albufera de Valencia. Biología de las aguas continentales II. Instituto Forestal de Investigaciones y Experiencias, Madrid.

Postel, S., Carpenter, S.R., 1997. Freshwater ecosystem services. In: Daily, G. (Ed.), Ecosystem Services. Island Press, Washington D.C.

Reynolds, C.S., 1984. The ecology of freshwater phytoplankton. first edition. Cambridge University Press, New York.

Reynolds, C.S., 2006. The ecology of phytoplankton. first edition. Cambridge University Press, New York.

Rodrigo, M.A., Alonso-Guillén, J.L., 2013. Assessing the potential of Albufera de València Lagoon sediments for the restoration of charophyte meadows. Ecol. Eng. 60, 445–452.

Romo, S., 1994. Growth parameters of *Pseudanabaena galeata* Böcher in culture under different light and temperature conditions. Arch. Hydrobiol. Suppl. Algol. Stud. 75, 239–248.

Romo, S., Miracle, M.R., 1993. Long-term periodcity of *Planktothrix agardhii*, *Pseudanabaena galeata* and *Geitlerinema* sp. in a shallow hypertrophic lagoon, the Albufera of Valencia (Spain). Arch. Hydrobiol. 126, 469–486.

Romo, S., Miracle, M.R., 1994. Population dynamics and ecology of subdominant phytoplankton species in a shallow hypertrophic lake (Albufera of Valencia, Spain). Hydrobiologia 273, 37–56.

Romo, S., Miracle, M.R., 1995. Diversity of the phytoplankton assemblages of a polymictic hypertrophic lake. Arch. Hydrobiol. 132, 363–384.

Romo, S., Miracle, M.R., et al., 2004. Mesocosm experiments on nutrient and fish effects on shallow lake food webs in a Mediterranean climate. Freshw. Biol. 49, 1593–1607.

Romo, S., Villena, M.J., Sahuquillo, M., Soria, J.M., Gimenez, M., Alfonso, T., Vicente, E., Miracle, M.R., 2005. Response of a shallow Mediterranean lake to nutrient diversion: does it follow similar patterns as in northern shallow lakes? Freshw. Biol. 50, 1706–1717.

Romo, S., García-Murcia, A., Villena, M.J., Balleste, V.S.A., 2008. Tendencias del fitoplancton en el lago de la Albufera de Valencia e implicaciones para su ecología, gestión y recuperación. Limnetica 27, 11–28.

Sahuquillo, M., Melão, M., Miracle, M., 2007. Low filtering rates of *Daphnia magna* in a hypertrophic lake: laboratory and in situ experiments using synthetic microspheres. Hydrobiologia 594, 141–152.

Sanz, M., Carratalá, A., Gimeno, C., Millán, M., 2002. Atmospheric nitrogen deposition on the east coast of Spain: relevance of dry deposition in semi-arid Mediterranean regions. Environ. Pollut. 118, 259–272.

Scheffer, M., Hosper, S.H., Meijer, M.L., Moss, B., Jeppesen, E., 1993. Alternative equilibria in shallow lakes. Trends Ecol. Evol. 8, 275–279.

Schindler, D.W., 2006. Recent advances in the understanding and management of eutrophication. Limnol. Oceanogr. 51, 356–363.

Schutten, J., Dainty, J., Davy, A., 2004. Wave-induced Hydraulic Forces on Submerged Aquatic Plants in Shallow Lakes. Ann. Bot. Lond. 93, 333–341.

Shoaf, T.W., Lium, B.W., 1976. Improved extraction of chlorophyll a and b from algae using dimethylsulphoxide. Limnol. Oceanogr. 21, 926–928.

Simon, M., Azam, F., 1989. Protein content and protein synthesis rates of planktonic marine bacteria. Mar. Ecol. Prog. Ser. 51, 201–213.

Smith, V.H., 2003. Eutrophication of freshwater and coastal marine ecosystems a global problem. Environ. Sci. Pollut. Res. 10, 126–139.

Smith, V.H., Joye, S.B., Howarth, R.W., 2006. Eutrophication of freshwater and marine ecosystems. Limnol. Oceanogr. 51, 351–355.

Sommaruga, R., 1995. Microbial and classical food webs: A visit to a hypertrophic lake. FEMS Microbiol. Ecol. 17, 257–270.

Sommer, U., 1989. Plankton Ecology, succession in plankton communities. Springer.

Søndergaard, M., Jensen, P.J., Jeppesen, E., 2001. Retention and internal loading of phosphorus in shallow, eutrophic lakes. Sci. World J. 1, 427–442.

Søndergaard, M., Jensen, J.P., Jeppesen, E., 2003. Role of sediment and internal loading of phosphorus in shallow lakes. Hydrobiologia 506, 135–145.

Søndergaard, M., Jensen, J.P., Jeppesen, E., 2005. Seasonal response of nutrients to reduced phosphorus loading in 12 Danish lakes. Freshw. Biol. 50, 1605–1615.

Soria, J., Vicente, E., 2002. Estudio de los aportes hídricos al parque natural de la Albufera de Valencia. Limnetica 21, 105–115.

Sterner, R.W., Elser, J.J., Hessen, D.O., 1992. Stoichiometric relationships among producers, consumers and nutrient cycling in pelagic ecosystems. Biogeochemistry 17, 49–67.

Stow, C.A., Roessler, C., Borsuk, M.E., Bowen, J.D., Reckhow, K.H., 2003. Comparison of estuarine water quality models for total maximum daily load development in Neuse River Estuary. J. Water Resour. Plan. ASCE 129, 307–314.

Telesh, I.V., Rahkola, M., Viljanen, M., 1998. Carbon content of some freshwater rotifers. Hydrobiologia 387, 355–360.

Tian, R.C., Vézina, A.F., Starr, M., Saucier, F., 2001. Seasonal dynamics of coastal ecosystems and export production at high latitudes: a modeling study. Limnol. Oceanogr. 46, 1845–1859.

Tirok, K., Gaedke, U., 2006. Spring weather determines the relative importance of ciliates, rotifers and crustaceans for the initiation of the clear-water phase in a large, deep lake. J. Plankton Res. 28, 361–373.

Tõnno, I., Künnap, H., Nõges, T., 2003. The role of zooplankton grazing in the formation of 'clear water phase' in a shallow charophyte-dominated lake. Hydrobiologia 506, 353–358.

Usaquén Perilla, O.L., Gómez, A.G., Gómez, A.G., Díaz, C.Á., Cortezón, J.A.R., 2012. Methodology to assess sustainable management of water resources in coastal lagoons with agricultural uses: An application to the Albufera lagoon of Valencia (Eastern Spain). Ecol. Indic. 13, 129–143.

Vicente, E., Miracle, M., 1992. The coastal lagoon Albufera de Valencia: An ecosystem under stress. Limnetica 8, 87–100.

Vicente, E., Soria, J.M., Peña, R., 2012. Fluxos hídrics, qualitat d'aigua i heterogeneïtat especial. In: Català, J. (Ed.), La universitat de València i els seus entorns naturals: els parcs naturals de l'Albufera, el Túria i la Serra Calderona. Universitat de València, València, pp. 92–95.

Villena, M.J., Romo, S., 2003. Phytoplankton changes in a shallow Mediterranean lake (Albufera of Valencia, Spain) after sewage diversion. Hydrobiologia 506, 281–287.

Wetzel, R.G., 1990. Land-water interfaces: metabolic and limnological regulators. Int. Ver. Theor. Angew. Limnol. 24, 6–24.

Wetzel, R., 2001. Limnology: Lake and River Ecosystems. third edition. Springer, San Diego.

Zhang, W., Rao, Y.R., 2012. Application of a eutrophication model for assessing water quality in Lake Winnipeg. J. Great Lakes Res. 38, 158–173.